The NLO jet vertex for Mueller-Navelet and forward jets: The quark part

J. Bartels⋆, D. Colferai⋆⋆, G.P. Vacca⋆

II. Institut für Theoretische Physik, Universität Hamburg, Luruper Chaussee 149, 22761 Hamburg, Germany

Abstract. We calculate the next-to-leading corrections to the jet vertex which is relevant for the Mueller-Navelet-jets production in $p\bar{p}$ collisions and for the forward jet cross section in ep collisions. In this first part we present the results of the vertex for an incoming quark. Particular emphasis is given to the separation of the collinear divergent part and the central region of the produced gluon.

1 Introduction

The BFKL Pomeron [1] presents the perturbative QCD prediction for the Pomeron, and in recent years attempts have been made to verify its relevance for experimental data. Apart from the $\gamma^*\gamma^*$ total cross section in e^+e^- scattering which is generally considered to be the gold-plated BFKL measurement [2], special jet measurements have been proposed both for hadron-hadron colliders (Mueller-Navelet jets [3]) and for deep inelastic scattering (forward jets [4]). First comparisons of the leading order calculations [5,6] with experimental data have clearly demonstrated the need of next-to-leading order calculations: both in the e^+e^- measurements at LEP and in DIS at HERA the data are below the leading $\log s$ (LL) curves, while data from the $p\bar{p}$ collider at TEVATRON are found above the LL estimates. The next-to-leading (NLL) corrections to the BFKL kernel [7,8] lower the theoretical prediction, but they are so large that they might even cause serious problems for the stability of the series. Various attempts [9,10] have been made in order to improve the predictivity of the NLL BFKL approach. However, so far one has not been able to perform a consistent NLL analysis of the data. First of all, a consistent NLL framework for describing not fully inclusive processes, such as jet observables, has not been established yet. In addition, even adopting the LL high energy factorization formulae at NLL level, a few important pieces of the NLL calculations are still missing.

The three measurements for searching high energy QCD dynamics are illustrated in Fig. 1: for a complete NLL analysis one needs, in addition to the NLL calculation of the BFKL kernel, the photon impact factor and the jet production vertex. Whereas the former one is cur-

rently being investigated by two groups [11,12], the latter one, so far, has not been calculated. It is the purpose of this paper to present a consistent factorization formula for high energy jet cross sections at NLL level, and to obtain first results for the jet vertex, namely the quark-initiated vertex. The case of an incoming gluon will be presented in a forthcoming paper [13].

The theoretical challenge in performing a NLL calculation of such a jet vertex is that it lies at the interface of collinear factorization and BFKL dynamics: in Fig. 1c the lower incoming parton emerges from the proton and produces a hard jet, thus obeying the rules of DGLAP evolution [14] and collinear factorization. Above the vertex, on the other hand, one requires a large separation in rapidity between the two outgoing jets (which are assumed to have large transverse energies of comparable magnitude). The kinematics between the jets, therefore, belongs to large-$\log s$ dynamics and is described in terms of the BFKL language. When computing next-to-leading (NLO) corrections[1] to the jet production vertex, one expects to find collinear divergencies which have to be counted as higher order corrections of the incoming parton density; at the same time, part of the NLO corrections will overlap with high energy gluon radiation between the two jets which belongs to the leading $\log s$ (LL) BFKL approximation. It is one of the main goals of our analysis to show that both types of contributions can successfully be identified and separated from the NLL jet vertex.

As the central part of our calculation we will compute, to order α_s^3, the high energy limit of the cross section of the processes $q + q \rightarrow q + X + jet$ (Fig. 2), where X may contain one gluon or quark. The LL approximation of the order $\mathcal{O}(\alpha_s^3 \log s/s_0)$ has been calculated before [15], we will present the NLL (constant in s) term $\mathcal{O}(\alpha_s^3)$. We will

---

[1] Note the difference between LL (leading $\log s$) and LO (lowest order) and that between NLL (next-to-leading $\log s$) and NLO (next-to-leading order = next-to-lowest order = one-loop)
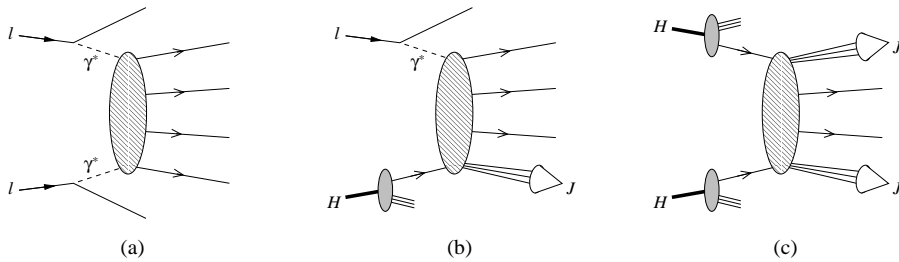
Fig. 1a–c. Schematic diagrams representing the three processes searching for high energy QCD dynamics: **a** double DIS or $\gamma^*\gamma^*$ scattering; **b** DIS with forward jet; **c** hadron-hadron scattering with dijets or Mueller-Navelet jets

show that the cross section can be written in a factorized form: there are NLL corrections to the impact factor of the upper incoming quark (which have been calculated before [16]), and for the emission of the gluon in the central region we recover the LL BFKL result. Finally, the NLL corrections to the jet vertex of the lower incoming quark are what we obtain as new result. Making use of this high energy factorizing, we can use our results for the Mueller-Navelet jets (Fig.1c): we can apply the NLL results not only to the lower jet vertex but also to the upper one. For the forward jets in DIS (Fig. 1b) we have the NLL corrections for the jet vertex, but we have to wait for the completion of the NLL corrections to the photon impact factor.

An important result of the NLL calculation is the dependence upon the energy scale s_0: in the leading $\log s$ approximation this scale is undetermined and thus introduces a principal uncertainty of the theoretical prediction. The NLL calculation determines how the cross section changes with a change in s_0 and removes this uncertainty.

Moreover, at next-to-leading order, the renormalized parton densities start to play a role, reducing drastically the dependence on the collinear factorization scale μ_F, otherwise maximal in all previous LO calculations.

Our paper will be organized as follows. We begin with a brief outline of our program. In Sects. 3 and 4 we present the results of our calculation: first the virtual corrections, then the real corrections. Our main emphasis will be on the separation of soft and collinear divergencies at the vertex of the lower incoming quark and on the removal of the central region of the produced gluon. Combining the real and virtual corrections we obtain in Sect. 5 an analytic expression for the jet vertex. We conclude with a brief summary and discussion.

2 High energy factorization

2.1 General framework

The processes that we are going to study are those in which a hadron H strongly interacts with parton b; to be definite, we chose b to be a quark. In the final state a jet J (in the forward direction with respect to H) is then identified (see Fig. 2). Our notation uses light cone coordinates

$$p^\mu = (p^+, p^-, \boldsymbol{p}) , \quad p^\pm := \frac{p^0 \pm p^3}{\sqrt{2}} , \qquad (1)$$
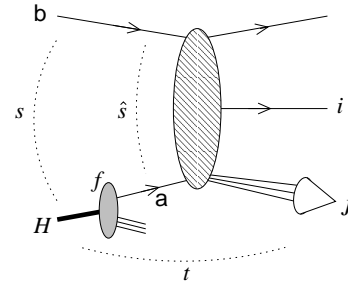
Fig. 2. Diagrammatic representation of the high energy process studied in this paper. H is the incoming hadron providing parton a with distribution density f; b is the other incoming particle which will be taken to be a quark; J denotes the jet produced in the forward direction (w.r.t H) and i is the generic label for outgoing particles

where the light-like vectors p_H and p_b form the basis of the longitudinal plane:

$$p_H = \left(\sqrt{\frac{s}{2}}, 0, \boldsymbol{0} \right) , \quad s := (p_H + p_b)^2 \qquad (2a)$$

$$p_b = \left(0, \sqrt{\frac{s}{2}}, \boldsymbol{0} \right) \qquad (2b)$$

$$p_i = E_i \left(\frac{\mathrm{e}^{y_i}}{\sqrt{2}}, \frac{\mathrm{e}^{-y_i}}{\sqrt{2}}, \boldsymbol{\phi}_i \right) . \qquad (2c)$$

In the last equation we have introduced a parameterization for the i-th particle in the final state in terms of the rapidity y_i (in the $p_H + p_b$ center of mass frame), of the transverse energy $E_i = |\boldsymbol{p}_i|$ and of the azimuthal unit vector $\boldsymbol{\phi}_i \parallel \boldsymbol{p}_i$.

As usual, our jet consists of a certain number of partons, whose rapidities and azimuthal angles are found inside a given (small) region in the (y, ϕ) plane. The position of the center of that region defines the rapidity y_J and the azimuthal angle ϕ_J of the jet, its size is related to the jet radius R, and the sum of the transverse energies of the particles forming the jet constitutes the jet transverse energy E_J. We will keep our jet definition rather general; it only has to obey a few minimal requirements (see Sect. 4.1).

We will be interested in the high energy limit of the subprocess $a + b \to q + i + jet$. In addition to the energy s, we need to define the momentum transfer

$$t := (p_H - p_J)^2 . \qquad (3)$$

and the jet energy E_J:

$$p_J \simeq E_J \left(\frac{\mathrm{e}^{y_J}}{\sqrt{2}}, \frac{\mathrm{e}^{-y_J}}{\sqrt{2}}, \phi_J \right) \quad \Longrightarrow \quad -t \simeq \sqrt{s} E_J \mathrm{e}^{-y_J}. \quad (4)$$

The high energy (Regge) limit that we are considering is defined by

$$E_J^2 \text{ fixed}, \quad t \text{ fixed}, \quad s \to \infty \quad (5)$$

which determines a logarithmic growth of the jet rapidity with s:

$$y_J \sim \tfrac{1}{2} \log s . \quad (6)$$

The use of perturbation theory is justified because we consider all kinematic scales much greater than the QCD scale:

$$E_J^2 \sim -t \gg \Lambda_{\mathrm{QCD}}^2; . \quad (7)$$

This condition allows also us to neglect the masses and the Fermi motion of the light partons inside H. Equivalently, in terms of the twist expansion, the leading twist contribution can be extracted by considering the parton massless and collinear to H. We shall therefore adopt

$$p_{\mathsf{a}} = x\, p_H = \left(x\sqrt{\frac{s}{2}}, 0, \mathbf{0} \right) . \quad (8)$$

It is well known that the Regge limit is dominated by gluon t-channel exchanges [1] and that, in the leading logarithmic approximation, the elastic scattering amplitude and the total cross section can be written in a factorizing form: (i) a gluon Green's function which describes the exchanged system, and (ii) impact factors which denote the coupling to the scattering partons or particles. NLO corrections that have been computed for the BFKL kernel [7,8] and for a few impact factors [16–19] support this factorizing form also in next-to-leading order. It is one of the goals of this paper to verify this factorization also for the inelastic process $\mathsf{a} + \mathsf{b} \to \mathsf{a} + i + jet$. Thanks to this property we will be able to treat, on the same footing, several classes of processes. Two of them are crucial for the study of QCD in the Regge limit:

- *dijet*, or Mueller-Navelet jets, coming from hadron-hadron collisions where a jet is detected in the forward direction of each hadron; in this case particle b is a hadron;
- *forward jet*, coming from lepton-hadron collisions where a jet is detected in the forward direction with respect to the hadron; in this case particle b is identified with the virtual gauge boson, e.g. a photon, emitted by the lepton.

In the following we assume that a proper definition of the jet has been chosen. This choice is represented by a function (actually a distribution) S_J which selects the final state configurations contributing to the observable we are interested in. The jet cross section is given by the action of S_J on the full exclusive cross section in $D = 4 + 2\varepsilon$ spacetime dimensions

$$\mathrm{d}\sigma = \frac{1}{2s} \sum_{n=2}^{\infty} (2\pi)^D \delta^D \left(p_H + p_{\mathsf{b}} - \sum_{i=2}^{n} p_i \right)$$
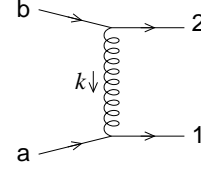
Fig. 3. Leading diagram at lowest order for parton-parton scattering: the interaction occurs via gluon exchange in the t-channel

$$\times \langle |\mathcal{M}_{H\mathsf{b} \to n}|^2 \rangle\, \mathrm{d}\Phi_n(p_1, \cdots, p_n) \quad (9)$$

as follows:

$$\frac{\mathrm{d}\sigma}{\mathrm{d}J} := \frac{\mathrm{d}\sigma}{\mathrm{d}y_J \mathrm{d}E_J \mathrm{d}\phi_J} = \int \mathrm{d}\sigma\, S_J . \quad (10)$$

Here $J = (y_J, E_J, \phi_J)$ collects the jet variables, n is the number of particles in the final state, $\mathcal{M}$ is the invariant amplitude and $\mathrm{d}\Phi$ is the phase space measure.

In order to describe perturbatively a hadron-initiated process, we assume – according to the parton model – the physical cross section to be given by the corresponding partonic cross section $\mathrm{d}\hat{\sigma}_{\mathsf{a}}$ (computable in perturbation theory) convoluted with the distribution densities f_{a} of the partons a inside the hadron H. The partonic distribution functions (PDFs) $f_{\mathsf{a}} : \mathsf{a} \in H$ constitute a non-perturbative input. This approach is justified provided the infrared singularities stemming from QCD interaction among massless objects can be consistently absorbed in a redefinition of the PDFs according to the well known factorization of mass singularities [20]. Those "renormalized PDFs" will be eventually interpreted as the universal objects measured in hadronic collisions and obeying the DGLAP equations. Let us therefore write

$$\mathrm{d}\sigma = \sum_{\mathsf{a} \in H} \int_0^1 \mathrm{d}x\, \mathrm{d}\hat{\sigma}_{\mathsf{b}\mathsf{a}}(x)\, f_{\mathsf{a}}^{(0)}(x) \quad (11)$$

where $x = p_{\mathsf{a}}^+ / p_H^+$ is the longitudinal momentum fraction of the parton a with respect to the parent hadron H. In (11) we show explicitly that, according to the previous discussion, the PDFs must still be considered as "bare" quantities. In conclusion, the jet cross section is given by

$$\frac{\mathrm{d}\sigma}{\mathrm{d}J} = \sum_{\mathsf{a}} \int \mathrm{d}x\, \mathrm{d}\hat{\sigma}_{\mathsf{b}\mathsf{a}}(x)\, S_J(x) f_{\mathsf{a}}^{(0)}(x) \quad (12)$$

and is diagrammatically represented in Fig. 2.

We proceed by reviewing parton-hadron scattering at lowest order.

2.2 The Jet vertex at lowest order

In order to evaluate the jet cross section in the high energy regime (5) for parton-hadron scattering, thanks to (12), we need only to consider parton-parton scattering. At lowest order (LO), the relevant cross section is dominated by one gluon exchange in the t-channel, as shown in Fig. 3. Let

us define the gluon momentum and the partonic center of mass energy squared

$$k := p_1 - p_a = -zp_a + wp_b + k_\perp , \quad k_\perp = (0,0,\boldsymbol{k}) , \quad (13)$$
$$\hat{s} := (p_a + p_b)^2 = xs .$$

The partonic cross section is constant in $\hat{s}$ and is given by

$$d\hat{\sigma}_{ba}^{(0)} = h_b^{(0)}(\boldsymbol{k})h_a^{(0)}(\boldsymbol{k})d\boldsymbol{k} , \quad d\boldsymbol{k} \equiv d^{2+2\varepsilon}\boldsymbol{k} , \quad (14)$$

in terms of the LO partonic impact factors [17]

$$h_i^{(0)}(\boldsymbol{k}) := \mathcal{N}\frac{C_i}{\boldsymbol{k}^2} ,$$
$$\mathcal{N} = \frac{2^{1+\varepsilon}\alpha_s}{\mu^{2\varepsilon}\Gamma(1-\varepsilon)\sqrt{N_c^2-1}} , \quad (i = a,b) , \quad (15)$$

where the colour factor C_i is $C_F = (N_c^2 - 1)/2N_c$ for a quark ($i = q$) and $C_A = N_c$ for a gluon ($i = g$); the coupling α_s in $D = 4 + 2\varepsilon$ dimensions is defined in (37).

It is evident that the jet can contain only one of the two particles in the final state, the other moving in the opposite direction. Furthermore, since we are looking for the jet in the forward direction with respect to H, the configuration $p_2 = p_J$ gives a negligible contribution to the cross section. This can be easily seen by noticing that the corresponding amplitude involves a propagator $\sim 1/|u| \simeq 1/s$ much smaller than that of the $p_1 = p_J$ amplitude $\sim 1/t$. This means that, at lowest order, the jet momentum has to be identified with p_1, so that the jet distribution for two-particle final states, according to (10), reads

$$S_J^{(2)}(p_1, p_2; p_a, p_b) = \delta(y_1 - y_J)\delta(E_1 - E_J)\delta(\phi_1 - \phi_J) . \quad (16)$$

As independent variables in $S_J^{(2)}$ we can adopt $\boldsymbol{p}_1 = \boldsymbol{k}$ for the final state, and $p_a^+/p_H^+ = x$ for the initial state, so that we can define

$$\mathcal{S}_J^{(2)}(\boldsymbol{k}; x) := S_J^{(2)}(p_1, p_2; p_a, p_b)$$
$$= \delta\left(1 - \frac{x_J}{x}\right)E_J^{1+2\varepsilon}\delta(\boldsymbol{k} - \boldsymbol{k}_J) ,$$
$$x_J := \frac{E_J e^{y_J}}{\sqrt{s}} , \quad (17)$$

being $\boldsymbol{k}_J$ the transverse momentum of the jet. By substituting (14) and (17) in (12), the LO jet cross section assumes the factorized form
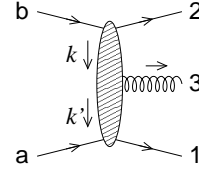
$$\frac{d\sigma^{(0)}}{dJ} = \sum_a \int dx \int d\boldsymbol{k}\, h_b^{(0)}(\boldsymbol{k})h_a^{(0)}(\boldsymbol{k})\mathcal{S}_J^{(2)}(\boldsymbol{k}; x)f_a^{(0)}(x) . \quad (18)$$

Besides the PDF f_a and the partonic impact factor h_b, we are left with a term that can be interpreted as the LO jet vertex
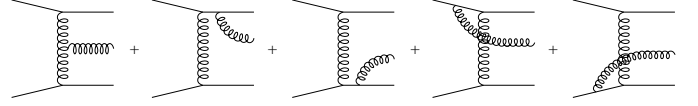
$$V_a^{(0)}(\boldsymbol{k}, x) := h_a^{(0)}(\boldsymbol{k})\mathcal{S}_J^{(2)}(\boldsymbol{k}; x) . \quad (19)$$

The lowest order formula for the jet cross section is therefore

$$\frac{d\sigma^{(0)}}{dJ} = \sum_a \int dx \int d\boldsymbol{k}\, h_b^{(0)}(\boldsymbol{k})V_a^{(0)}(\boldsymbol{k}, x)f_a^{(0)}(x) . \quad (20)$$

Fig. 4. Labelling the two-to-three parton scattering process. Note the definition of the transferred momenta k and k'

Fig. 5. Feynman diagrams contributing to the $qq \to qqg$ process at leading log s order

2.3 One-loop analysis: LL approximation and future strategy

Moving on to higher order, let us first address the leading logarithmic approximation, i.e., terms of the order $\alpha_s^n \log^n(s/-t)$. The resummation of these terms, also referred to as leading logarithmic (LL) approximation, was addressed long ago for fully inclusive processes [1], and it has also been applied to dijets [5] and forward jets [6]. It is instructive to review briefly how the logarithmic enhanced terms arise at one-loop, and to study the structure of the singularities and their connection with the various kinematic regions.

We consider first the real corrections to, say, quark-quark scattering, which involves the emission of an additional gluon of momentum p_3 as shown in Fig. 4. The structure of the final states giving the leading contributions corresponds to the so called multi-Regge kinematics (MRK)

$$y_1 \gg y_3 \gg y_2 , \quad E_1 \sim E_3 \sim E_2 , \quad (21)$$

where the rapidity y_3 of the emitted gluon is strongly ordered between the rapidities of the scattered partons y_1 and y_2 (i.e., the gluon is emitted in the central region), while the magnitudes of the transverse momenta are of the same order.

All diagrams shown in Fig. 5 contribute at LL, and the resulting differential partonic cross section reads

$$d\hat{\sigma}_{ba}^{(1,real)} \simeq \alpha_s h_b^{(0)}(\boldsymbol{k})h_a^{(0)}(\boldsymbol{k}')\frac{C_A}{\pi}\frac{1}{\pi_\varepsilon(\boldsymbol{k}-\boldsymbol{k}')^2}d\boldsymbol{k}\,d\boldsymbol{k}'\frac{dz}{z} , \quad (22)$$

where π_ε is given in (54). We have introduced the momenta transferred by the a and b partons

$$k := p_b - p_2 = -\bar{w}p_a + wp_b + k_\perp ,$$
$$k_\perp = (0,0,\boldsymbol{k}) \quad (23a)$$
$$k' := p_1 - p_a = -zp_a + \bar{z}p_b + k'_\perp ,$$
$$k'_\perp = (0,0,\boldsymbol{k}') . \quad (23b)$$

The transverse energies introduced in (2c) correspond to $E_1 = |\boldsymbol{k}'|, E_2 = |\boldsymbol{k}|, E_3 = |\boldsymbol{k} - \boldsymbol{k}'|$. In the MRK (21), $\bar{w} \sim \bar{z} \ll w \sim z \ll 1$, so that the outgoing parton 1
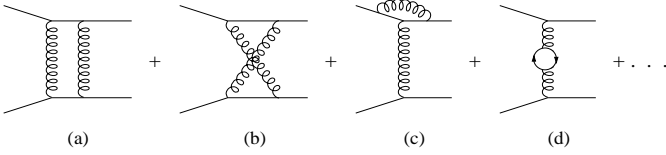
Fig. 6a–d. Feynman diagrams contributing to the one-loop virtual corrections to $qq \to qq$ elastic scattering in LL approximation **a,b** and in NLL approximation **c,d,...**

carries most of the plus-component of the parent parton a. By using (2c) and comparing with (8) we get

$$y_1 \simeq \log \frac{x\sqrt{s}}{E_1} . \qquad (24)$$

Since $E_1 = |\boldsymbol{k}'|$, $\boldsymbol{k}'$ characterizes completely the momentum p_1. The range of the momentum fraction z is approximately given by $\boldsymbol{p}_3^2/\hat{s} < z < 1 - \boldsymbol{k}'^2/\hat{s}$. The boundary values of z correspond to the gluon in the fragmentation region of parton b and a respectively, where (22) no longer holds. Nevertheless, it shows that, upon z-integration, a logarithmic factor $\log(\hat{s}/s_0)$ appears:

$$
\begin{aligned}
d\hat{\sigma}_{ba}^{(1,\text{real})} &= \int dz \, \frac{d\hat{\sigma}_{ba}^{(1,\text{real})}}{dz} \\
&= \alpha_s h_b^{(0)}(\boldsymbol{k}) h_a^{(0)}(\boldsymbol{k}') \qquad (25) \\
&\quad \times \left[K^{(0,\text{real})}(\boldsymbol{k}, \boldsymbol{k}') \log \frac{\hat{s}}{s_0} + \text{const} \right] d\boldsymbol{k} \, d\boldsymbol{k}'
\end{aligned}
$$

$$K^{(0,\text{real})}(\boldsymbol{k}, \boldsymbol{k}') := \frac{C_A}{\pi} \frac{1}{\pi_\varepsilon (\boldsymbol{k} - \boldsymbol{k}')^2} . \qquad (26)$$

The coefficient of the $\log s$ term $K^{(0,\text{real})}$ is the real part of the leading log BFKL kernel. The *scale of the energy* s_0 is a parameter of the order of the transverse momenta squared of the gluons ($s_0 \sim \boldsymbol{p}_3^2 = |\boldsymbol{k} - \boldsymbol{k}'|^2 \sim \boldsymbol{k}^2 \sim \boldsymbol{k}'^2$). Its value is not determined in the LL approximation – a change of s_0 would affect only the constant piece in (25) –, but will play a central role when going to the next-to-leading level of accuracy. In particular, that part of the differential cross section in which the emitted gluon lies outside the central region contributes to the constant term (i.e., without a $\log s$ enhancement).

Let us now consider the virtual corrections. In covariant gauges, the diagrams involving two gluon exchanges (see Figs. 6a,b) give contributions to the amplitude which increase logarithmically with the energy, whereas other diagrams (shown in Figs. 6c,d) have no logarithmic enhancement. Note, however, that the latter diagrams contain the ultra-violet (UV) singularities that provide the renormalization of the coupling.

The result of the virtual correction to the partonic cross section can be presented as follows:

$$d\hat{\sigma}_{ba}^{(1,\text{virt})} = \alpha_s h_b^{(0)}(\boldsymbol{k}) h_a^{(0)}(\boldsymbol{k}) \left[2\omega^{(1)}(\boldsymbol{k}) \log \frac{\hat{s}}{\boldsymbol{k}^2} + \text{const} \right] d\boldsymbol{k}. \qquad (27)$$

The coefficient $\omega^{(1)}$ in front of the $\log s$ is the *one-loop Regge-gluon trajectory*, because – according to Regge the-

ory – the amplitude for $ab \to ab$ elastic scattering mediated by color octet exchange is described by the exchange of a reggeized gluon and takes the form:

$$\mathcal{M}_{ba} \sim \left(\frac{s}{-t} \right)^{\omega(t)} = 1 + \alpha_s \omega^{(1)}(t) \log \frac{s}{-t} + \cdots . \qquad (28)$$

By taking the square modulus and adjusting the normalization through the LO expression (14), it is straightforward to match (27). This contribution to the cross section defines the virtual part of the LL BFKL kernel:

$$K^{(0,\text{virt})}(\boldsymbol{k}, \boldsymbol{k}') := 2\omega^{(1)}(\boldsymbol{k})\delta(\boldsymbol{k} - \boldsymbol{k}') . \qquad (29)$$

Together with (22) and (27) we obtain the full one-loop partonic cross section

$$
\begin{aligned}
d\hat{\sigma}_{ba}^{(1)} &= \alpha_s h_b^{(0)}(\boldsymbol{k}) h_a^{(0)}(\boldsymbol{k}') \\
&\quad \times \left[K^{(0)}(\boldsymbol{k}, \boldsymbol{k}') \log \frac{\hat{s}}{s_0} + \text{const} \right] d\boldsymbol{k} \, d\boldsymbol{k}' . \qquad (30)
\end{aligned}
$$

Here $K^{(0)}$ collects the real and virtual coefficients of the logarithmic terms:

$$K^{(0)}(\boldsymbol{k}, \boldsymbol{k}') := K^{(0,\text{real})}(\boldsymbol{k}, \boldsymbol{k}') + K^{(0,\text{virt})}(\boldsymbol{k}, \boldsymbol{k}') . \qquad (31)$$

and defines the LL BFKL kernel; the term *const* contains contributions that have no large energy logarithm.

Let us use these results to define the jet cross section. The jet we want to observe includes the outgoing particles carrying the largest values of rapidity lying within a specified (small) range R. However, the strong rapidity order in (21) allows only p_1 to enter the jet, so that the jet distribution for three particles in the final state $S_J^{(3)}$ reduces to the lowest order one $S_J^{(2)}$ (16) which, combined with the impact factor $h_a^{(0)}$ in (30), reproduces the lowest order jet vertex $V_a^{(0)}$ (19). Convoluting with the PDF we obtain the following factorized expression for the one-loop LL jet cross section ($\hat{s} = xs$):

$$
\begin{aligned}
\frac{d\sigma^{(1,\text{LL})}}{dJ} &= \alpha_s \sum_a \int dx \int d\boldsymbol{k} \, d\boldsymbol{k}' \, h_b^{(0)}(\boldsymbol{k}) K^{(0)}(\boldsymbol{k}, \boldsymbol{k}') \\
&\quad \times \log \frac{xs}{s_0} V_a^{(0)}(\boldsymbol{k}', x) f_a^{(0)}(x) . \qquad (32)
\end{aligned}
$$

It is the purpose of this paper to compute, in this order of α_s, the constant (i.e., non-logarithmic) corrections to our jet cross section formula. We generalize the results (20) and (32) and make the following *ansatz*:

$$
\begin{aligned}
\frac{d\sigma}{dJ} &= \alpha_s \sum_a \int dx \int d\boldsymbol{k} \, d\boldsymbol{k}' \, h_b(\boldsymbol{k}) \\
&\quad \times G(xs, \boldsymbol{k}, \boldsymbol{k}') V_a(\boldsymbol{k}', x) f_a(x) , \qquad (33a)
\end{aligned}
$$

$$G(xs, \boldsymbol{k}, \boldsymbol{k}') := \delta(\boldsymbol{k} - \boldsymbol{k}') + \alpha_s K^{(0)}(\boldsymbol{k}, \boldsymbol{k}') \log \frac{xs}{s_0} , \quad (33b)$$

According to the previous remarks, we suppose that the inclusion of the one-loop constant terms just provides perturbative corrections to the quark impact factor, to the jet vertex, and to the PDF as follows:

$$h = h^{(0)} + \alpha_s h^{(1)} \qquad (34a)$$

$$V = V^{(0)} + \alpha_{\mathrm{s}} V^{(1)} \tag{34b}$$

$$f = f^{(0)} + \alpha_{\mathrm{s}} f^{(1)} . \tag{34c}$$

Equivalently, our ansatz corresponds to the following structure for the one-loop cross section:

$$
\begin{aligned}
\frac{\mathrm{d}\sigma^{(1)}}{\mathrm{d}J} = {}& \alpha_{\mathrm{s}} \sum_{\mathsf{a}} \int \mathrm{d}x \int \mathrm{d}\boldsymbol{k} \Big\{ \int \mathrm{d}\boldsymbol{k}' \Big[h_{\mathsf{b}}^{(0)}(\boldsymbol{k}) K^{(0)}(\boldsymbol{k}, \boldsymbol{k}') \\
& \times \log \frac{xs}{s_0} V_{\mathsf{a}}^{(0)}(\boldsymbol{k}', x) f_{\mathsf{a}}^{(0)}(x) \Big] \\
& + h_{\mathsf{b}}^{(1)}(\boldsymbol{k}) V_{\mathsf{a}}^{(0)}(\boldsymbol{k}, x) f_{\mathsf{a}}^{(0)}(x) \\
& + h_{\mathsf{b}}^{(0)}(\boldsymbol{k}) V_{\mathsf{a}}^{(0)}(\boldsymbol{k}, x) f_{\mathsf{a}}^{(1)}(x) \\
& + h_{\mathsf{b}}^{(0)}(\boldsymbol{k}) V_{\mathsf{a}}^{(1)}(\boldsymbol{k}, x) f_{\mathsf{a}}^{(0)}(x) \Big\} ,
\end{aligned}
\tag{35}
$$

which is obtained simply by expanding (33a) up to relative order α_{s}.

In (35) the Born approximations (marked by the superscript (0)) have been listed in (15), (31), and (19) respectively. For the first order correction to the partonic impact factor, $h^{(1)}$, which appears on the second line, we can use the known expression of [16,17], and for the correction to the PDF, $f^{(1)}$, we have the usual convolution with the LO Altarelli-Parisi splitting functions:

$$
\begin{aligned}
\alpha_{\mathrm{s}} f_{\mathsf{a}}^{(1)}(x, \mu_F^2) :={}& \frac{\alpha_{\mathrm{s}}}{2\pi} \frac{1}{\varepsilon} \left(\frac{\mu_F^2}{\mu^2} \right)^{\varepsilon} \sum_{\mathsf{c}} \int_x^1 \frac{\mathrm{d}\xi}{\xi} P_{\mathsf{ac}}(\xi) f_{\mathsf{c}}^{(0)}\left(\frac{x}{\xi} \right) \\
={}& \frac{\alpha_{\mathrm{s}}}{2\pi} \frac{1}{\varepsilon} \left(\frac{\mu_F^2}{\mu^2} \right)^{\varepsilon} \sum_{\mathsf{c}} P_{\mathsf{ac}} \otimes f_{\mathsf{c}}^{(0)} .
\end{aligned}
\tag{36}
$$

Because of the definition (37) for $\alpha_{\mathrm{s}} = g^2 \mu^{2\varepsilon}/4\pi \left[1 + \varepsilon(\gamma_E - \log 4\pi)\right]$, (36) defines the one-loop PDF in the $\overline{\mathrm{MS}}$ scheme. Finally, the correction term $V_{\mathsf{a}}^{(1)}$ is what we want to compute in this paper.

Equations (33) and (34) constitute a highly non trivial ansatz, which will be shown to depend upon a careful separation of singular and finite pieces. Our main task will consist to identify the collinear singularities (36) which go into the renormalization of the parton densities, to check that the other infrared singularities cancel out when adding virtual and real corrections, and, finally, to separate the terms proportional to $\log s$ which belong into the first line of (35). At the end, a finite term remains, which eventually can be interpreted as one-loop correction to the jet vertex, $V_{\mathsf{a}}^{(1)}$.

In the rest of this paper we will compute this jet vertex correction, $V_{\mathsf{a}}^{(1)}$. In this paper we will concentrate on the case of incoming quark ($\mathsf{a} = \mathsf{q}$). The case of an incoming gluon ($\mathsf{a} = \mathsf{g}$) will be dealt with in a subsequent paper [13].

3 Virtual corrections

In the following we will develop the one-loop analysis of the quark-initiated jet production process. We adopt dimensional regularization in $D = 4 + 2\epsilon$ dimensions and

define, according to the $\overline{\mathrm{MS}}$ scheme, the dimensionless coupling α_{s} as a function of the dimensionful bare coupling g and of the renormalization scale μ as follows:

$$\alpha_{\mathrm{s}} = \alpha_{\mathrm{s}}^{(0)} := \frac{g^2 \mu^{2\varepsilon} \Gamma(1 - \varepsilon)}{(4\pi)^{1+\varepsilon}} \tag{37}$$

We begin by collecting the virtual corrections. Some of the diagrams are shown in Fig. 6. Discarding all terms suppressed by powers of s, the one-loop parton-parton cross section can be derived from [21] and reads

$$
\begin{aligned}
\mathrm{d}\hat{\sigma}_{\mathsf{ba}} = {}& \alpha_{\mathrm{s}} h_{\mathsf{b}}^{(0)}(\boldsymbol{k}) h_{\mathsf{a}}^{(0)}(\boldsymbol{k}) \\
& \times \left[2\omega^{(1)}(\boldsymbol{k}) \log \frac{xs}{\boldsymbol{k}^2} + \Pi_{\mathsf{b}}(\boldsymbol{k}) + \Pi_{\mathsf{a}}(\boldsymbol{k}) \right] \mathrm{d}\boldsymbol{k} .
\end{aligned}
\tag{38}
$$

The first term has already been introduced in Sect. 2.3: it represents the LL contribution to the virtual corrections. In particular the coefficient of $\log s$, namely $2\omega^{(1)}$, constitutes the virtual part of the leading kernel $K^{(0)}$ of (31) and is just twice the one-loop Regge-gluon trajectory

$$\omega^{(1)}(\boldsymbol{k}) = -\frac{C_A}{\pi} \frac{1}{2\varepsilon} \frac{\Gamma^2(1+\varepsilon)}{\Gamma(1+2\varepsilon)} \left(\frac{\boldsymbol{k}^2}{\mu^2} \right)^{\varepsilon} . \tag{39}$$

It shows an ε-pole due to a soft singularity which compensates the corresponding one of the real part of the kernel.

The non logarithmic terms in (38) represent the NLL contribution to the virtual corrections and are expressed in terms of the virtual corrections to the impact factor Π. The virtual corrections to the quark impact factor read:

$$
\begin{aligned}
\Pi_{\mathsf{q}}(\boldsymbol{k}) = {}& \left[-\frac{11N_c - 2N_f}{12\pi} \frac{1}{\varepsilon} + \left(\frac{85}{36} + \frac{\pi^2}{4} \right) \frac{C_A}{\pi} - \frac{5}{18} \frac{N_f}{\pi} \right. \\
& \left. - \left(\frac{1}{\varepsilon^2} - \frac{3}{2\varepsilon} + 4 - \frac{\pi^2}{6} \right) \frac{C_F}{\pi} \right] \left(\frac{\boldsymbol{k}^2}{\mu^2} \right)^{\varepsilon} .
\end{aligned}
\tag{40}
$$

In the above expression we have singled out terms of different physical origin. The first term is proportional to the β-function coefficient $b_0 = (11N_c - 2N_f)/12\pi$. It multiplies the ultraviolet (UV) pole providing the $\overline{\mathrm{MS}}$ renormalization of the coupling

$$\alpha_{\mathrm{s}}(\boldsymbol{k}^2) := \alpha_{\mathrm{s}}^{(0)} \left[1 - \alpha_{\mathrm{s}}^{(0)} \frac{b_0}{\varepsilon} \left(\frac{\boldsymbol{k}^2}{\mu^2} \right)^{\varepsilon} \right] . \tag{41}$$

In fact, at LO the partonic cross section (14) is simply the product of two bare partonic impact factors

$$\frac{\mathrm{d}\hat{\sigma}_{\mathsf{bq}}^{(0)}}{\mathrm{d}\boldsymbol{k}} = h_{\mathsf{b}}^{(0)}(\alpha_{\mathrm{s}}^{(0)}) h_{\mathsf{q}}^{(0)}(\alpha_{\mathrm{s}}^{(0)}) , \tag{42}$$

where we have explicitly shown only the dependence on $\alpha_{\mathrm{s}}^{(0)}$. Adding the UV divergent term of (38) stemming from Π_{q} renormalizes the coupling inside h_{q}:

$$\frac{\mathrm{d}\hat{\sigma}_{\mathsf{bq}}^{(0)}}{\mathrm{d}\boldsymbol{k}} + \frac{\mathrm{d}\hat{\sigma}_{\mathsf{bq}}^{(1,\mathrm{UV})}}{\mathrm{d}\boldsymbol{k}} \bigg|_{\Pi_{\mathsf{q}}} = h_{\mathsf{b}}^{(0)}(\alpha_{\mathrm{s}}^{(0)}) h_{\mathsf{q}}^{(0)}(\alpha_{\mathrm{s}}^{(0)}) \left[1 - \alpha_{\mathrm{s}}^{(0)} \frac{b_0}{\varepsilon} \right]$$

$$= h_{\mathsf{b}}^{(0)}(\alpha_{\mathsf{s}}^{(0)}) \, h_{\mathsf{q}}^{(0)}(\alpha_{\mathsf{s}}(\mu^2)) \,. \qquad (43)$$

The same UV pole can be found in Π_{b}, and it provides the running of the coupling of $h_{\mathsf{b}}^{(0)}$.

The virtual contribution to the jet cross section is easily obtained by substituting in (12) the expression (17) for the jet distribution and (38) for the partonic cross section. By combining the jet distribution with the quark q impact factor at LO we reproduce the LO jet vertex (19) and, after renormalization, we end up with

$$\frac{\mathrm{d}\sigma^{(\mathrm{virt})}}{\mathrm{d}J} = \alpha_{\mathsf{s}} \int \mathrm{d}x \int \mathrm{d}\boldsymbol{k} \, h_{\mathsf{b}}^{(0)}(\boldsymbol{k})$$
$$\times \left[2\omega^{(1)}(\boldsymbol{k}) \log \frac{xs}{\boldsymbol{k}^2} + \widetilde{\Pi}_{\mathsf{b}}(\boldsymbol{k}) + \widetilde{\Pi}_{\mathsf{q}}(\boldsymbol{k}) \right]$$
$$\times V_{\mathsf{q}}^{(0)}(\boldsymbol{k}, x) f_{\mathsf{q}}^{(0)}(x) \,, \qquad (44)$$

where

$$\widetilde{\Pi}_{\mathsf{q}}(\boldsymbol{k}) := \Pi_{\mathsf{q}}(\boldsymbol{k}) - (-b_0/\varepsilon)$$
$$= \left[\left(\frac{85}{36} + \frac{\pi^2}{4} \right) \frac{C_A}{\pi} - \frac{5}{18} \frac{N_f}{\pi} \qquad (45) \right.$$
$$\left. - \left(\frac{1}{\varepsilon^2} - \frac{3}{2\varepsilon} + 4 - \frac{\pi^2}{6} \right) \frac{C_F}{\pi} - b_0 \log \frac{\boldsymbol{k}^2}{\mu^2} \right] \left(\frac{\boldsymbol{k}^2}{\mu^2} \right)^{\varepsilon} \,.$$

Any occurrence of α_{s} in (44) and in all other coming formulae is to be understood as $\alpha_{\mathsf{s}}(\mu^2)$.

The "reduced" quark impact factor virtual correction (45) shows double and single poles in ε. These poles are of IR origin and are due to both soft and collinear singularities. Partly they will cancel against the corresponding singularities of the real emission corrections, leaving a simple pole that will be absorbed in the redefinition of the PDFs. This will be shown in Sect. 5.

4 Real corrections

When calculating the real emission corrections to the one-loop jet cross section, our main concern will be the correct treatment of the IR singularities (keeping in mind that we are considering a partially exclusive process). Infrared singularities are contained in the upper quark impact factor, the real part of the BFKL kernel, and in the lower jet vertex. Some of the latter ones contribute to the renormalization of the incoming parton density. *A priori* it is not evident that the overlap of the various regions of the phase space responsible for the divergencies can be disentangled in such a way that they reproduce all the expected singularities (and not more). We will show that this is actually the case.

4.1 Jet definition

We begin with a brief review of the jet definition. We follow the arguments given in [22], and we wish to keep our distribution functions $S_J^{(n)}$ as general as possible. In

massless QCD two kinds of IR singularities exist: *(i)* soft singularities which arise when a gluon is emitted with vanishing momentum; *(ii)* collinear singularities which arise when two interacting partons are emitted collinearly. In order to define infrared finite jet cross sections we have to require finite limits whenever momenta in the final state belong to either *(i)* or *(ii)*. Given a set of functions $S_J^{(n)}(p_1, \cdots, p_n; p_{\mathsf{a}}, p_{\mathsf{b}})$ (where $(p_{\mathsf{a}}, p_{\mathsf{b}})$ denote the momenta of the initial state), we have to require that a state $(p_1, \cdots, p_j, \cdots, p_n)$ with a soft particle $p_j \to 0$ be indistinguishable from the $n-1$-particle state $(p_1, \cdots, p_n)$:

$$\lim_{p_j \to 0} S_J^{(n)}(\cdots, p_j, \cdots; p_{\mathsf{a}}, p_{\mathsf{b}}) = S_J^{(n-1)}(\cdots; p_{\mathsf{a}}, p_{\mathsf{b}})$$
$$(46a)$$

with p_j being dropped in the RHS. In the same way, the n-particle state $(p_1, \cdots, p_i, p_{i+1}, \cdots, p_n)$ with two collinear particles, e.g. $p_i \parallel p_{i+1}$, cannot be distinguished from the $n-1$-particle final state $(p_1, \cdots, p_i + p_{i+1}, \cdots, p_n)$. The jet function must then fulfill

$$S_J^{(n)}(\cdots, ap, bp, \cdots; p_{\mathsf{a}}, p_{\mathsf{b}}) \qquad (46b)$$
$$= S_J^{(n-1)}(\cdots, (a+b)p, \cdots; p_{\mathsf{a}}, p_{\mathsf{b}}) \,, \quad (a, b > 0) \,.$$

When an outgoing particle is collinear to an incoming one, say a, a similar relation (which can be inferred from (46b) by invoking crossing symmetry) holds:

$$S_J^{(n)}(\cdots, ap_{\mathsf{a}}, \cdots; p_{\mathsf{a}}, p_{\mathsf{b}}) \qquad (46c)$$
$$= S_J^{(n-1)}(\cdots; (1-a)p_{\mathsf{a}}, p_{\mathsf{b}}) \,, \quad (0 < a < 1) \,.$$

The last equation expresses the property of factorizability of initial state collinear singularities. Equations (46b) and (46c) should be understood as smooth limits for momenta approaching the collinear configuration.

In our case real emission involves three partons in the final states, one gluon in addition to the incoming quarks a and b: abg. As indicated in Fig. 4, we label the outgoing partons in our process $\mathsf{ab} \to 123$ by $1 = (\text{quark a})$, $2 = (\text{quark b})$, and $3 = (\text{gluon g})$. Let us start by listing the possible IR singular configurations. Only the emission of gluon 3 with vanishing momentum gives rise to soft singularities. Collinear singularities arise in collinear emissions of partons that couple directly to each other, i.e., have a common vertex. This is the case for pairs of gluons, for quarks and gluons, and for identical incoming and outgoing quarks (or quarks and antiquarks). Therefore, the list of all possible collinear singular configurations, in an obvious notation, reads as follows:

$$\mathsf{a} \parallel 1 \,, \qquad \mathsf{a} \parallel 3 \,, \qquad 1 \parallel 3 \,, \qquad (47a)$$
$$\mathsf{b} \parallel 2 \,, \qquad \mathsf{b} \parallel 3 \,, \qquad 2 \parallel 3 \,. \qquad (47b)$$

It is important to note that, in the kinematic regime we are considering, configurations in which quark 2 is emitted outside the fragmentation region of quark b are strongly suppressed, i.e., quark 2 never belongs to the jet produced in the forward direction of quark a. To see this we note that as long as quark b is deflected at small angles by gluon

exchange, the amplitude contains a $1/t$ factor coming from the gluon propagator. Suppose, on the other hand, quark b deflected with an angle large enough to enter the central region or even the fragmentation region of quark a (which includes the jet region). If the scattering happens by gluon exchange, the propagator of the latter is of order $1/|u| \simeq 1/s$, providing a suppression factor $\sim t/s$ compared to the small angle case. There is also the possibility of quark exchange that involves a $1/t$ propagator, but in this case the spin of the quark introduces a new suppression factor $\sim \sqrt{-t/s}$ compared to the gluon exchange. Therefore, we can safely neglect the configurations in which quark 2 enters the jet, and only particles 1 and 3 play a role in building up the jet.

To become more specific, we change the argument structure of the jet distribution functions $S_J^{(n=3)}$ and introduce, as independent variables, $\boldsymbol{p}_1, \boldsymbol{p}_3, p_3^+, p_{\mathsf{a}}^+$:

$$\mathcal{S}_J^{(3)}\left(\boldsymbol{p}_1, \boldsymbol{p}_3, \frac{p_3^+}{p_H^+}; \frac{p_{\mathsf{a}}^+}{p_H^+}\right) \equiv \mathcal{S}_J^{(3)}(\boldsymbol{k}', \boldsymbol{k} - \boldsymbol{k}', xz; x)$$
$$:= S_J^{(3)}(p_1, p_2, p_3; p_{\mathsf{a}}, p_{\mathsf{b}}) . \quad (48)$$

The soft IR constraint (46a) of $S_J^{(3)}$ applies only to soft gluon emission and, since quark 2 does not participate in the jet, the collinear conditions (46b,c) apply only to the configurations listed in (47a). The corresponding relations for $\mathcal{S}_J^{(3)}$ read:

$$3 \text{ soft} : \quad \mathcal{S}_J^{(3)}(\boldsymbol{p}, \boldsymbol{0}, 0; x) = \mathcal{S}_J^{(2)}(\boldsymbol{p}; x) \quad (49a)$$

$$1 \parallel 3 : \quad \mathcal{S}_J^{(3)}(a\boldsymbol{p}, b\boldsymbol{p}, \xi; x) = \mathcal{S}_J^{(2)}((a+b)\boldsymbol{p}; x) \quad (49b)$$

$$\mathsf{a} \parallel 1 : \quad \mathcal{S}_J^{(3)}(\boldsymbol{0}, \boldsymbol{p}, \xi; x) = \mathcal{S}_J^{(2)}(\boldsymbol{p}; \xi) \quad (49c)$$

$$\mathsf{a} \parallel 3 : \quad \mathcal{S}_J^{(3)}(\boldsymbol{p}, \boldsymbol{0}, \xi; x) = \mathcal{S}_J^{(2)}(\boldsymbol{p}; x - \xi) . \quad (49d)$$

In the following sections these relations will be used when extracting the divergencies of the real emission. It is crucial that the singular contributions generated by the real corrections are proportional to the LO cross section: only in this case cancellations with the virtual singularities can occur, and the factorization of the collinear singularities into the PDFs can be performed consistently. Therefore, the reduction $\mathcal{S}_J^{(3)} \to \mathcal{S}_J^{(2)}$ in the IR singular configurations contained in (49) is a necessary prerequisite.

4.2 Phase space splitting and the master formula

Before embarking in the analysis of the one-loop real corrections, let us divide the phase space of the outgoing gluon and present the 'master formula' that we are going to make use of. We have already pointed out that the log s term arises from the configurations with gluon 3 emitted in the central region, while the gluon in the fragmentation region of b should mainly contribute to the impact factor correction $h_{\mathsf{b}}^{(1)}$ whereas the gluon in the fragmentation region of q should provide the jet vertex $V_{\mathsf{q}}^{(1)}$ and the PDF corrections $f_{\mathsf{q}}^{(1)}$. It is easy to define a rapidity cut that separates the two fragmentation regions: we

perform a boost into the positive z-direction which takes us into the partonic center of mass system (PCMF). It shifts rapidities while transverse energies and azimuthal angles are preserved. Consequently, a four momentum p^μ is transformed into p'^μ with

$$p'^\mu = (p'^+, p'^-, \boldsymbol{p}') = (\mathrm{e}^{\Delta y} p^+, \mathrm{e}^{-\Delta y} p^-, \boldsymbol{p}) ,$$
$$\Delta y = \frac{1}{2} \log \frac{1}{x} , \quad (50)$$

and rapidity is shifted according to $y' = y + \Delta y$. In the PCMF, we define the cut as the rapidity center $y'_{\mathrm{cut}} = 0$ which corresponds to $y_{\mathrm{cut}} = -\frac{1}{2} \log \frac{1}{x}$. In the Sudakov parameterization (23), the form of the cut is very simple:

$$y_3 = y'_{\mathrm{cut}} = 0 \quad \Longleftrightarrow \quad w_{\mathrm{cut}} = z_{\mathrm{cut}} = \frac{E_3}{\sqrt{xs}} . \quad (51)$$

Correspondingly, our rapidity phase space is divided into the "upper half region" (negative rapidity: $y'_3 < 0$ or $w > \frac{E_3}{\sqrt{xs}}$) which contains the fragmentation region of quark b and half of the central region, and the "lower half region" (positive rapidity: $y'_3 > 0$ or $z > \frac{E_3}{\sqrt{xs}}$) which contains the other half of the central region and the fragmentation of parton q and contributes to the jet vertex.

Finally, we need the partonic differential cross section for the bq $\to$ 123 process. They have been computed in [16, 17]. In the high energy regime, where we neglect terms suppressed by powers of s, the form of the partonic differential cross section turns out to be quite simple when restricted to one of the two halves of the phase space, $y'_3 < 0$ or $y'_3 > 0$. For the "lower half region" $y'_3 > 0$ the cross section can be cast into the general form

$$\mathrm{d}\hat{\sigma}_{\mathsf{ba} \to fin} = h_{\mathsf{b}}^{(0)}(\boldsymbol{k}) F_{fin}(\boldsymbol{k}, \boldsymbol{k}', z) h_{\mathsf{a}}^{(0)}(\boldsymbol{k}') \, \mathrm{d}\boldsymbol{k} \, \mathrm{d}\boldsymbol{k}' \, \mathrm{d}z ,$$
$$(z > z_{\mathrm{cut}}) , \quad (52)$$

where the function F depends on the particular final state. In particular, for quark-quark scattering, we have

$$F_{\mathsf{qqg}}(\boldsymbol{k}, \boldsymbol{k}', z) = \frac{\alpha_s}{2\pi} \frac{\mathcal{P}_{\mathsf{gq}}(z, \varepsilon)}{\pi_\varepsilon} \frac{1}{\boldsymbol{q}^2 (\boldsymbol{q} - z\boldsymbol{k})^2} \quad (53)$$
$$\times \left[C_F z^2 \boldsymbol{k}'^2 + C_A (1-z) \boldsymbol{q} \cdot (\boldsymbol{q} - z\boldsymbol{k}) \right] ,$$

$$\mathcal{P}_{\mathsf{gq}}(z, \varepsilon) = \frac{1 + (1-z)^2 + \varepsilon z^2}{z} ,$$
$$\pi_\varepsilon = \pi^{1+\varepsilon} \Gamma(1-\varepsilon) \mu^{2\varepsilon} , \quad (54)$$

where $\boldsymbol{q} = \boldsymbol{k} - \boldsymbol{k}'$ is the gluon transverse momentum and $\mathcal{P}_{\mathsf{gq}}(z, \varepsilon)$ is – apart from a missing C_F factor – the real part of the q $\to$ g splitting function in $4 + 2\varepsilon$ dimensions. In the "upper half region" $y'_3 < 0$, the same relation (52) holds with the replacements

$$\boldsymbol{k} \to -\boldsymbol{k}' , \quad \boldsymbol{k}' \to -\boldsymbol{k} , \quad \boldsymbol{q} \to \boldsymbol{q} , \quad z \to w , \quad (55)$$

except for the impact factor which retain their form. These 'master formulae' (53)–(55) will be used in the following in order to find the real corrections to the quark-initiated jet vertex.
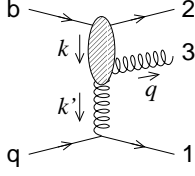
Fig. 7. Structure of the Feynman diagrams contributing to the $\mathsf{qb} \to \mathsf{qbg}$ process in NLL approximation when the outgoing gluon is emitted with negative rapidity $y_3' < 0$. The blob represents all possible $\mathsf{bg}^* \to \mathsf{bg}$ QCD sub-diagrams

4.3 Real corrections to the upper quark impact factor

We begin by computing the contribution to the jet cross section given by the "upper half region" $y_3' < 0$ which gives rise to the NLO impact factor of the upper quark. The starting formula is derived from (12), using (48) for the jet distribution (with $z = E_3^2/wxs$ to good accuracy) and (52) and (53) (with the replacements (55)) for the partonic cross section:

$$
\begin{aligned}
\frac{d\sigma^{(y_3'<0)}}{dJ} = & \frac{\alpha_{\mathrm{s}}}{2\pi} \int d\boldsymbol{k}\, d\boldsymbol{k}'\, h_{\mathsf{b}}^{(0)}(\boldsymbol{k}) h_{\mathsf{q}}^{(0)}(\boldsymbol{k}') \\
& \times \int_{w_{\mathrm{cut}}}^1 dw\, \frac{\mathcal{P}_{\mathsf{gq}}(w,\varepsilon)}{\pi_\varepsilon} \frac{1}{\boldsymbol{q}^2(\boldsymbol{q}+w\boldsymbol{k}')^2} \\
& \times \left[C_F w^2 \boldsymbol{k}^2 + C_A(1-w)\boldsymbol{q}\cdot(\boldsymbol{q}+w\boldsymbol{k}') \right] \\
& \times \int_0^1 dx\, \mathcal{S}_J^{(3)}\left(\boldsymbol{k}',\boldsymbol{q},\frac{E_3^2}{wxs}x;x\right) f_{\mathsf{q}}^{(0)}(x)\,.\ (56)
\end{aligned}
$$

Since $y_3 < y_3' < 0$, the gluon is emitted very far from the jet region $y \simeq y_J \pm R$, for which $y_J \sim \log\sqrt{s} \gg R \sim 1$ (cf. (6)). Therefore, only quark 1 can enter the jet, so that in this half of the phase space

$$
\begin{aligned}
\mathcal{S}_J^{(3)}\left(\boldsymbol{k}',\boldsymbol{q},\frac{E_3^2}{wxs}x;x\right) &= \mathcal{S}_J^{(3)}\left(\boldsymbol{k}',\boldsymbol{q},\frac{E_3^2}{ws};x\right) \qquad (57) \\
&= \mathcal{S}_J^{(2)}(\boldsymbol{k}';x)\,, \quad (w > w_{\mathrm{cut}})\,.
\end{aligned}
$$

It is now possible to factor out from the w and $\boldsymbol{k}$ integrals the q impact factor and the jet distribution, which, according to (19), reproduce the LO jet vertex. We obtain:

$$
\frac{d\sigma^{(y_3'<0)}}{dJ} = \alpha_{\mathrm{s}} \int dx \int d\boldsymbol{k}'\, U(\boldsymbol{k}',x) V_{\mathsf{q}}^{(0)}(\boldsymbol{k}',x) f_{\mathsf{q}}^{(0)}(x),
\tag{58}
$$

$$
\begin{aligned}
U(\boldsymbol{k}',x) := & \frac{\mathcal{N}C_F}{2\pi} \int \frac{d\boldsymbol{k}}{\pi_\varepsilon \boldsymbol{k}^2} \int_{w_{\mathrm{cut}}}^1 \frac{dw}{w} \left[1+(1-w)^2+\varepsilon w^2\right] \\
& \times \frac{C_F w^2 \boldsymbol{k}^2 + C_A(1-w)\boldsymbol{q}\cdot(\boldsymbol{q}+w\boldsymbol{k}')}{\boldsymbol{q}^2(\boldsymbol{q}+w\boldsymbol{k}')^2}\,.\ (59)
\end{aligned}
$$

The computation of the U integral can be done following the calculation of [16]. We repeat here the main steps. Let us consider separately the two terms involving different colour constants.

The integrand of the C_F term of U is regular – actually vanishes – for $w \to 0$ at fixed $\boldsymbol{k}$, so that the lower bound

w_{cut} can be set equal to zero, introducing a negligible error of order E_3^2/s. Changing the transverse integration variable $\boldsymbol{k} \to \boldsymbol{q} = \boldsymbol{k} - \boldsymbol{k}'$ yields

$$
\begin{aligned}
U_{C_F} \simeq & \frac{\mathcal{N}C_F^2}{2\pi} \int_0^1 dw\, w \left[1+(1-w)^2+\varepsilon w^2\right] \\
& \times \int \frac{d\boldsymbol{q}}{\pi_\varepsilon} \frac{1}{\boldsymbol{q}^2(\boldsymbol{q}+w\boldsymbol{k}')^2}\,.\ (60)
\end{aligned}
$$

Until now, we have not mentioned any upper limit of the transverse momentum integrations. We know that the transverse momentum squared of the outgoing particles are kinematically limited to some value of the order of s. For our purposes, however, these upper limits are not important, because the transverse momentum integrals converge in the ultraviolet region $\boldsymbol{k} \to \infty$, and extending the upper limit of integration to infinity causes negligible errors of order $1/s$:

$$
\int_{|\boldsymbol{q}|\sim\sqrt{s}}^\infty \frac{d\boldsymbol{q}}{\boldsymbol{q}^4} \propto \int_s^\infty \frac{dt}{t^2} = \frac{1}{s}\,.
\tag{61}
$$

The transverse integral in (60) can then be easily performed,

$$
\begin{aligned}
& \int \frac{d\boldsymbol{q}}{\pi_\varepsilon} \frac{1}{\boldsymbol{q}^2(\boldsymbol{q}+w\boldsymbol{k}')^2} \\
& = \frac{w^{2\varepsilon-2}}{\boldsymbol{k}'^2} \left(\frac{\boldsymbol{k}'^2}{\mu^2}\right)^\varepsilon \frac{\Gamma^2(\varepsilon)}{\Gamma(2\varepsilon)} \\
& = \frac{w^{2\varepsilon-2}}{\boldsymbol{k}'^2} \left(\frac{\boldsymbol{k}'^2}{\mu^2}\right)^\varepsilon 2\left[\frac{1}{\varepsilon} - \frac{\pi^2}{6}\varepsilon + \mathcal{O}(\varepsilon^2)\right]\,.\ (62)
\end{aligned}
$$

The ε pole reflects the two collinear singularities at $\boldsymbol{q} = 0$ and $\boldsymbol{q} + w\boldsymbol{k}' = 0$ which correspond to $\mathsf{b} \parallel 3$ and $2 \parallel 3$, respectively. At this point also the w-integration can be easily performed. Because of the pre-factor $w^{2\varepsilon-2}$ in (62), the w-integration turns out to be divergent[2] at $w = 0$. This is just the soft singularity expected for $p_3 \to 0$. The final result for U_{C_F} is

$$
U_{C_F} = \frac{C_F}{\pi} h_{\mathsf{b}}^{(0)}(\boldsymbol{k}') \left(\frac{\boldsymbol{k}'^2}{\mu^2}\right)^\varepsilon \left[\frac{1}{\varepsilon^2} - \frac{3}{2\varepsilon} + 4 - \frac{\pi^2}{6}\right]
\tag{63}
$$

up to terms $\mathcal{O}(\varepsilon)$. For the impatient reader we note that the whole U_{C_F} cancels out when added to the virtual corrections of Sect. 3.

The C_A term of U requires special care, because it contributes to the high energy leading $\log s$ piece of the cross section. In Sect. 2.3 (22) we have presented the leading partonic differential cross section, which is nothing but the partonic cross section (52) with (53) evaluated in the

---

[2] The reader could object that the $w = 0$ singularity is an artifact of having set $w_{\mathrm{cut}} = 0$ which corresponds to having neglected an infinite contribution. However this procedure is consistent in that the logic of this calculation is first to perform the Regge limit (5) at $\varepsilon \neq 0$ and only as a last step, after cancellation of the divergencies, to perform the physical $\varepsilon \to 0$ limit

$z \to 0$ limit (the central region). The same consideration holds also here after the replacements (55). In particular we identify the leading term of U_{C_A} with

$$
U_{C_A}^{\mathrm{LL}} = \frac{\mathcal{N} C_A C_F}{\pi} \int \frac{\mathrm{d}\boldsymbol{k}}{\pi_\varepsilon \boldsymbol{k}^2} \frac{1}{(\boldsymbol{k}-\boldsymbol{k}')^2} \int_{w_{\mathrm{cut}}}^1 \mathrm{d}w \, \frac{\vartheta(w,\boldsymbol{k},\boldsymbol{k}')}{w}
$$

$$
= 2\pi \int \mathrm{d}\boldsymbol{k}\, h_{\mathsf{b}}^{(0)}(\boldsymbol{k}) K^{(0,\mathrm{real})}(\boldsymbol{k},\boldsymbol{k}')
$$

$$
\times \int_{w_{\mathrm{cut}}}^1 \mathrm{d}w \, \frac{\vartheta(w,\boldsymbol{k},\boldsymbol{k}')}{w} \,, \tag{64}
$$

where $K^{(0,\mathrm{real})}$ is defined in (26). The function ϑ in the above equation signals that the functional form of the integrand, accurate in the central region, has to break down somewhere in the fragmentation region of quark b. According to the analysis of [23], the emission probability in the splitting $\mathsf{q} \to \mathsf{q}'\mathsf{g}$ is dynamically suppressed when the emission angle of the gluon g is smaller than that of the quark q'. In the present case, by comparing the ratios of transverse to longitudinal components of particles 2 and 3, one expects the active phase space to be

$$
\frac{E_3}{w} > \frac{E_2}{1-w} \quad \Longleftrightarrow \quad w < \frac{E_3}{E_2 + E_3} \,. \tag{65}
$$

This has led the author of [16] to propose a leading term of the form of (64) with $\vartheta(w,\boldsymbol{k},\boldsymbol{k}') := \Theta(E_3 - wE_2)$, which matches (65) in the low-w region. With this choice,

$$
U_{C_A}^{\mathrm{LL}} = \int \mathrm{d}\boldsymbol{k}\, h_{\mathsf{b}}^{(0)}(\boldsymbol{k}) K^{(0,\mathrm{real})}(\boldsymbol{k},\boldsymbol{k}') \log \frac{\sqrt{xs}}{r(\boldsymbol{k},\boldsymbol{k}')} \tag{66}
$$

$$
r(\boldsymbol{k},\boldsymbol{k}') = \max(E_2, E_3) \,.
$$

The remaining part of U_{C_A}, i.e., $U_{C_A} - U_{C_A}^{\mathrm{LL}}$, is constant in s, and hence it is a NLL contributions; it is given by an integral that, at fixed transverse momenta, is now finite for $w_{\mathrm{cut}} \to 0$. The result is

$$
U_{C_A}^{\mathrm{NLL}} = \frac{C_A}{\pi} h_{\mathsf{b}}^{(0)}(\boldsymbol{k}') \left(\frac{\boldsymbol{k}'^2}{\mu^2}\right)^\varepsilon \left[-\frac{3}{4\varepsilon} - \frac{\pi^2}{3} - \frac{1}{4} \right] \,. \tag{67}
$$

The ε-pole stems from the transverse $\boldsymbol{k}$-integration in the neighbourhood of the singularity at $\boldsymbol{k} = 0$.

The complete contribution of the "upper half region" to the jet cross section can be conveniently presented if combined with the virtual correction contribution of (44) coming from the b impact factor correction $\widetilde{\Pi}_{\mathsf{b}}$:

$$
\frac{\mathrm{d}\sigma^{(y_3' < 0)}}{\mathrm{d}J} + \frac{\mathrm{d}\sigma^{(\mathrm{virt})}}{\mathrm{d}J}\bigg|_{\widetilde{\Pi}_{\mathsf{b}}}
$$

$$
= \alpha_{\mathsf{s}} \int \mathrm{d}x \int \mathrm{d}\boldsymbol{k}\, \mathrm{d}\boldsymbol{k}'\, h_{\mathsf{b}}^{(0)}(\boldsymbol{k}) K^{(0,\mathrm{real})}(\boldsymbol{k},\boldsymbol{k}')
$$

$$
\times \log \frac{\sqrt{xs}}{\max(E_2,E_3)} V_{\mathsf{q}}^{(0)}(\boldsymbol{k}',x) f_{\mathsf{q}}^{(0)}(x) \tag{68a}
$$

$$
+ \alpha_{\mathsf{s}} \int \mathrm{d}x \int \mathrm{d}\boldsymbol{k}\, h_{\mathsf{b}}^{(1)}(\boldsymbol{k}) V_{\mathsf{q}}^{(0)}(\boldsymbol{k},x) f_{\mathsf{q}}^{(0)}(x) \,, \tag{68b}
$$

In addition to a LL part, this formula reproduces the first constant term of (35) (of course, only the term $\mathsf{a} = \mathsf{q}$),

namely the full one-loop impact factor correction of the upper quark b:

$$
h_{\mathsf{b}}^{(1)}(\boldsymbol{k}) = \frac{C_A}{\pi} \left[\left(-\frac{3}{4} + \frac{\varepsilon}{4}\right) \frac{1}{\varepsilon} + \frac{67}{36} - \frac{\pi^2}{12} - \frac{5N_f}{18C_A} \right]
$$

$$
\times \left(\frac{\boldsymbol{k}^2}{\mu^2}\right)^\varepsilon - b_0 \log \frac{\boldsymbol{k}^2}{\mu^2} \,. \tag{69}
$$

The quark impact factor has been calculated also in [18], but there a different definition has been used. In order to explain the relation between the two approaches, some general remarks on the definition of impact factors and energy scales might be in place. It is known that processes involving coloured incoming particles are affected by collinear singularities that lead to divergent cross sections. These singularities depend on the type of the incoming particles, and it is therefore natural to associate them with the process dependent impact factors. In our paper, we follow [16,17], and we require *the partonic impact factors to include singularities of collinear origin only*. Such a prescription may sound somewhat academic, because partonic impact factors have no phenomenological application and interpretation. However, in view of the jet vertex which in the present paper represents our main goal, this requirement is very natural.

Namely, at the lower end of the diagram, where the coupling of the reggeized gluon to the incoming parton is described by the jet vertex (more precisely, by the convolution $V_{\mathsf{a}} \otimes f_{\mathsf{a}}$ which we may call "jet impact factor") it is mandatory that its singularity structure matches the one required by collinear factorization. Only in this case f_{a} can be identified as the usual parton density with one-loop corrections (36), and only with this prescription the remaining jet vertex V_{a} is finite. As we shall see in the next section, the jet distribution function helps to disentangle this structure from the leading log part in a very natural way, but the basic requirement is the matching of the singularity structure with the collinear singularities.

In our approach we therefore insist on the collinear properties of any impact factor. It is apparent from (69) that $h_{\mathsf{b}}^{(1)}$ has a simple pole which is the one expected from the $\mathsf{b} \parallel 2$ collinear divergence – more precisely, the residue of the pole reproduces the non singular part of the γ_{gq} anomalous dimension. This is a consequence of our choice for the LL subtraction needed to define the impact factor: the angular ordering prescription takes proper account of the whole neighbourhood of the $\mathsf{b} \parallel 2$ collinear region, and it avoids spurious singularities which potentially could be present due to the $(\boldsymbol{k}-\boldsymbol{k}')^2$ denominator in (64). Nevertheless, even with this requirement on the singularity structure there is still some freedom in the definition of the impact factor – essentially a factorization-scheme arbitrariness – which corresponds to changes in its finite (in ε) part. It is possible to show that the "good" collinear properties of the impact factors are preserved, provided the angular ordering prescription in the leading term is fulfilled in the soft (small w, E_3) region, while the details of the subtraction at finite w or E_3 affect only the finite part.

Returning to the evaluation of leading term, one might think of two different strategies. First, we could consider the whole $U_{C_A}^{\mathrm{LL}}$ term as part of the kernel: this amounts to perform the w-integral in (64) and to obtain the LL kernel, multiplied by a logarithm of the energy. This corresponds to the first line of (66), where the energy scale r (the denominator in the argument of the log), being a function of $\boldsymbol{k}$ and $\boldsymbol{k}'$, is determined by the particular LL subtraction, i.e., by ϑ. If we adopt, for instance, the angular ordering prescription in the whole range of w, i.e., $\vartheta(w, \boldsymbol{k}, \boldsymbol{k}') := \Theta(E_3 - w(E_2 + E_3))$, the energy scale is $r = E_2 + E_3$. In this case the new impact factor differs from (69) only by a finite piece.

Alternatively, we might chose a particular energy scale, say $\bar{r}$, and then decompose $U_{C_A}^{\mathrm{LL}}$ into a leading term containing the $\log(\sqrt{xs}/\bar{r})$, plus a next-to-leading term containing the $\log(r/\bar{r})$. The latter term can be expressed, at relative order $\mathcal{O}(\alpha_{\mathrm{s}})$, as a multiplicative operator factor:

$$(h^{(0)} + \alpha_{\mathrm{s}} h^{(1)})(1 + \alpha_{\mathrm{s}} H_L^{(\bar{r})}) \left(1 + \alpha_{\mathrm{s}} K^{(0)} \log \frac{\sqrt{xs}}{\bar{r}}\right) \quad (70)$$

$$H_L^{(\bar{r})}(\boldsymbol{k}, \boldsymbol{k}') := K^{(0)}(\boldsymbol{k}, \boldsymbol{k}') \log \frac{\bar{r}(\boldsymbol{k}, \boldsymbol{k}')}{r(\boldsymbol{k}, \boldsymbol{k}')} . \quad (71)$$

As long as we have chosen the energy scale $\bar{r}$ in such a way that in the limit $\boldsymbol{k} \ll \boldsymbol{k}'$ ($\boldsymbol{k} - \boldsymbol{k}' \ll \boldsymbol{k}$) it reduces to $\bar{r} \to |\boldsymbol{k}'| \simeq |\boldsymbol{k} - \boldsymbol{k}'| = E_3$ ($\bar{r} \to |\boldsymbol{k}| = E_2$), the factor $(1 + \alpha_{\mathrm{s}} H_L)$ can be safely embodied in the impact factor term without spoiling its collinear properties, i.e., it changes $h^{(1)}$ only by a finite (in ε) amount.

On the other side, for Regge-motivated scales of the energy like the one proposed in [7], the inclusion of the H_L term in the impact factors[3] leads to a different infrared behaviour, giving rise even to double poles. In this case, in our opinion, it will be useful to separate the factor $(1 + \alpha_{\mathrm{s}} H_L)$ from the impact factor and eventually to include it into the definition of the NLO BFKL kernel.

4.4 Real corrections to the jet vertex

In this section we consider the real corrections in the "lower half region" $y_3' > 0$, i.e., the corrections to the jet vertex. The starting formula is derived from (12), using (48) for the jet distribution and (52) and (53) for the partonic cross section:

$$\frac{\mathrm{d}\sigma^{(y_3' > 0)}}{\mathrm{d}J} = \frac{\alpha_{\mathrm{s}}}{2\pi} \mathcal{N} C_F \int \mathrm{d}\boldsymbol{k}\, \mathrm{d}\boldsymbol{k}'\, h_{\mathsf{b}}^{(0)}(\boldsymbol{k})$$
$$\times \int_{z_{\mathrm{cut}}}^1 \mathrm{d}z\, \frac{\mathcal{P}_{\mathsf{gq}}(z, \varepsilon)}{\pi_\varepsilon} \frac{1}{\boldsymbol{k}'^2 \boldsymbol{q}^2 (\boldsymbol{q} - z\boldsymbol{k})^2}$$
$$\times \left[C_F z^2 \boldsymbol{k}'^2 + C_A(1 - z)\boldsymbol{q} \cdot (\boldsymbol{q} - z\boldsymbol{k})\right]$$
$$\times \int_0^1 \mathrm{d}x\, \mathcal{S}_J^{(3)}(\boldsymbol{k}', \boldsymbol{q}, xz; x) f_{\mathsf{q}}^{(0)}(x) , \quad (72)$$

---

[3] In [18], one can find the expression for the impact factor at the Regge-scale $\bar{r} = |\boldsymbol{k}'| = E_2$ and the equivalence with our expression $(h^{(0)} + h^{(1)})(1 + \alpha_{\mathrm{s}} H_L^{(\bar{r})})$ is proven
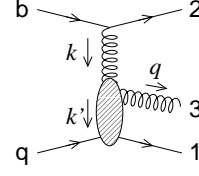
Fig. 8. Structure of the Feynman diagrams contributing to the $\mathsf{qb} \to \mathsf{qbg}$ process in NLL approximation when the outgoing gluon is emitted with positive rapidity $y_3' > 0$. The blob represents all possible $\mathsf{qg}^* \to \mathsf{qg}$ QCD sub-diagrams

where we have used (15) in order to write explicitly the kinematic dependence of the q impact factor.

In this phase space region, the quark-quark $\{\mathsf{b}, 2\}$ subsystem is kinematically well separated from the quark-quark-gluon $\{\mathsf{q}, 1, 3\}$ system, and they are connected only via the exchange of a gluon of momentum k (Fig. 8). Therefore, at fixed k, the dynamics of the two subsystems are independent of each other. Actually, because of the $\boldsymbol{k}$-factorization [24], only the transverse momentum $\boldsymbol{k}$ and the longitudinal component w need to be fixed in order to separate the two systems, because the $\{\mathsf{b}, 2\}$ system does not contain final state emissions at large sub-energies, and its dependence on the longitudinal component $\bar{w}$ is very weak and can be neglected. Moreover, the value of w is constrained by the mass-shell condition of quark 2, so that only $\boldsymbol{k}$ is the relevant variable between the two subsystems. We therefore expect a "pure" $\boldsymbol{k}$-factorization, where the $\{\mathsf{b}, 2\}$ coupling with the exchanged gluon is described simply by the $h_{\mathsf{b}}^{(0)}(\boldsymbol{k})$ impact factor. In order to find the expression for the $\{\mathsf{q}, 1, 3\}$ system and its coupling to the gluon (and to the hadron H), we fix the transverse momentum $\boldsymbol{k}$, remove the b impact factor and study the remaining part of the jet cross section (72).

First of all, it is important to understand the structure of the singularities in (72). The integrand contains three singular points in the $\boldsymbol{k}'$-integration, namely the zeroes of the denominator $\boldsymbol{k}' = 0$, $\boldsymbol{q} = 0$, and $\boldsymbol{q} - z\boldsymbol{k} = 0$. These points correspond to the collinear configurations $\mathsf{q} \parallel 1$, $\mathsf{q} \parallel 3$ and $1 \parallel 3$, respectively. Moreover, there is a potential soft singularity hidden in the $1/z$ pole of the "splitting function" $\mathcal{P}_{\mathsf{gq}}$. The numerators in the square brackets of (72) soften some of those singularities, but this happens differently for the C_F and the C_A parts. Therefore, we consider these two terms separately.

4.4.1 C_F term

The C_F term, owing to the $\boldsymbol{k}'^2$ factor in the numerator, has no $\mathsf{q} \parallel 1$ collinear singularity. Due to the factor z^2 in the numerator, the z-integrand is no longer singular at $z = 0$ and, along the same line of arguments as given in Sect. 4.3, we can shift the value of $z_{\mathrm{cut}} \to 0$. Dropping the $(y_3' > 0)$ label, the C_F part of (72) is given by

$$\frac{\mathrm{d}\sigma^{C_F}}{\mathrm{d}J} = \alpha_{\mathrm{s}} \frac{\mathcal{N} C_F^2}{2\pi} \int \mathrm{d}\boldsymbol{k}\, h_{\mathsf{b}}^{(0)}(\boldsymbol{k}) \int_0^1 \mathrm{d}x\, f_{\mathsf{q}}^{(0)}(x)$$

$$\times \int_0^1 \mathrm{d}z \, z^2 \mathcal{P}_{\mathsf{gq}}(z,\varepsilon) \int \frac{\mathrm{d}\boldsymbol{k}'}{\pi_\varepsilon} \frac{1}{\boldsymbol{q}^2(\boldsymbol{q}-z\boldsymbol{k})^2}$$
$$\times \mathcal{S}_J^{(3)}(\boldsymbol{k}',\boldsymbol{q},xz;x) \,. \tag{73}$$

It is convenient to rescale the gluon transverse momentum by setting $\boldsymbol{q} =: z\boldsymbol{l}$, and to use $\boldsymbol{l}$ as integration variable by substituting $\boldsymbol{k}' = \boldsymbol{k} - z\boldsymbol{l}$, so that $\boldsymbol{q} - z\boldsymbol{k} = z(\boldsymbol{l} - \boldsymbol{k})$. Next we perform a simple fraction decomposition in order to separate the initial (i) state $(\mathsf{q} \parallel 3 \iff \boldsymbol{l} = 0)$ and final (f) state $(1 \parallel 3 \iff \boldsymbol{l} - \boldsymbol{k} = 0)$ collinear singularities:

$$\frac{1}{\boldsymbol{l}^2(\boldsymbol{l}-\boldsymbol{k})^2} = \frac{1}{\boldsymbol{l}^2+(\boldsymbol{l}-\boldsymbol{k})^2}\left[\frac{1}{\boldsymbol{l}^2}+\frac{1}{(\boldsymbol{l}-\boldsymbol{k})^2}\right] \,. \tag{74}$$

Beginning with the **final state** (f) collinear singularity, in terms of the new variables the C_F contribution to the jet cross section can be rewritten in the form

$$\frac{\mathrm{d}\sigma}{\mathrm{d}J}_{C_F}^{f} := \alpha_{\mathsf{s}} \int_0^1 \frac{\mathrm{d}z}{z^{1-2\varepsilon}} \int \frac{\mathrm{d}\boldsymbol{l}}{\pi_\varepsilon(\boldsymbol{l}-\boldsymbol{k})^2} I(z,\boldsymbol{l})$$
$$= \frac{\mathrm{d}\sigma}{\mathrm{d}J}_{C_F}^{f,\text{soft}} + \frac{\mathrm{d}\sigma}{\mathrm{d}J}_{C_F}^{f,\text{coll}} + \frac{\mathrm{d}\sigma}{\mathrm{d}J}_{C_F}^{f,\text{finite}} \,, \tag{75}$$

which is particularly suitable for the analytic extraction of the divergencies: the RHS contains three pieces, $1)$ the soft divergence, $2)$ a pure collinear divergence, and $3)$ a finite part. The explicit expression of the integrand I in (75) is

$$I(z,\boldsymbol{l}) := \frac{C_F}{2\pi} z \mathcal{P}_{\mathsf{gq}}(z,\varepsilon) \int \mathrm{d}\boldsymbol{k} \, h_{\mathsf{b}}^{(0)}(\boldsymbol{k}) \frac{\mathcal{N}C_F}{\boldsymbol{l}^2+(\boldsymbol{l}-\boldsymbol{k})^2}$$
$$\times \int_0^1 \mathrm{d}x \, \mathcal{S}_J^{(3)}(\boldsymbol{k}-z\boldsymbol{l}, z\boldsymbol{l}, xz;x) f_{\mathsf{q}}^{(0)}(x) \,. \tag{76}$$

The soft term in (75) is defined by evaluating the integrand in the soft limit $z \to 0$. In this limit, the jet distribution can be simplified by means of (49a), and leads to the constraint $\boldsymbol{k}^2 = E_J^2$. One obtains

$$\frac{\mathrm{d}\sigma}{\mathrm{d}J}_{C_F}^{f,\text{soft}} := \alpha_{\mathsf{s}} \int_0^1 \frac{\mathrm{d}z}{z^{1-2\varepsilon}} \int \frac{\mathrm{d}\boldsymbol{l}}{\pi_\varepsilon(\boldsymbol{l}-\boldsymbol{k})^2} I(0,\boldsymbol{l})$$
$$= \alpha_{\mathsf{s}} \frac{C_F}{\pi} \int \mathrm{d}\boldsymbol{k} \, h_{\mathsf{b}}^{(0)}(\boldsymbol{k}) \int_0^1 \frac{\mathrm{d}z}{z^{1-2\varepsilon}}$$
$$\times \int \frac{\mathrm{d}\boldsymbol{l}}{\pi_\varepsilon(\boldsymbol{l}-\boldsymbol{k})^2} \frac{\mathcal{N}C_F}{\boldsymbol{l}^2+(\boldsymbol{l}-\boldsymbol{k})^2}$$
$$\times \int_0^1 \mathrm{d}x \, \mathcal{S}_J^{(2)}(\boldsymbol{k};x) f_{\mathsf{q}}^{(0)}(x)$$
$$= \alpha_{\mathsf{s}} \frac{C_F}{\pi}\left[\frac{1}{2\varepsilon^2} - \frac{\pi^2}{12} + \mathcal{O}(\varepsilon)\right]\left(\frac{E_J^2}{\mu^2}\right)^\varepsilon \int \mathrm{d}\boldsymbol{k}$$
$$\times \int_0^1 \mathrm{d}x \, h_{\mathsf{b}}^{(0)}(\boldsymbol{k}) V_{\mathsf{q}}^{(0)}(\boldsymbol{k},x) f_{\mathsf{q}}^{(0)}(x) \,, \tag{77}$$

where, in the final result, we have collected some factors in such a way that they reproduce the LO jet vertex (19). It can easily be seen that we have recovered the LO structure of the factorization formula. The additional divergent factor exhibits single as well as double poles, because our definition of the soft part includes also the region where collinear and soft singularities merge.

The pure collinear singularity can be isolated by evaluating the integrand (76) in the collinear limit $\boldsymbol{l} = \boldsymbol{k}$, after having subtracted the soft term $(\boldsymbol{l} = \boldsymbol{k}, z = 0)$. The resulting expression is clearly regular in the soft limit $(z \to 0)$ and therefore contains a simple collinear pole. An UV cutoff Λ is introduced since the residue at the collinear limit is no more integrable in the UV region. Thanks to (49b) the jet distribution simplifies to $\mathcal{S}_J^{(2)}$:

$$\frac{\mathrm{d}\sigma}{\mathrm{d}J}_{C_F}^{f,\text{coll}} := \alpha_{\mathsf{s}} \int_0^1 \frac{\mathrm{d}z}{z^{1-2\varepsilon}} \int \frac{\mathrm{d}\boldsymbol{l}}{\pi_\varepsilon(\boldsymbol{l}-\boldsymbol{k})^2}\left[I(z,\boldsymbol{k}) - I(0,\boldsymbol{k})\right]$$
$$\times \Theta(\Lambda^2 - (\boldsymbol{l}-\boldsymbol{k})^2)$$
$$= \alpha_{\mathsf{s}} \frac{C_F}{2\pi} \int \mathrm{d}\boldsymbol{k} \, h_{\mathsf{b}}^{(0)}(\boldsymbol{k}) \frac{\mathcal{N}C_F}{\boldsymbol{k}^2}$$
$$\times \int_0^1 \frac{\mathrm{d}z}{z^{1-2\varepsilon}}\left[z\mathcal{P}_{\mathsf{gq}}(z,\varepsilon) - 2\right]$$
$$\times \int \frac{\mathrm{d}\boldsymbol{l}}{\pi_\varepsilon(\boldsymbol{l}-\boldsymbol{k})^2}\Theta(\Lambda^2 - (\boldsymbol{l}-\boldsymbol{k})^2)$$
$$\times \int_0^1 \mathrm{d}x \, \mathcal{S}_J^{(2)}(\boldsymbol{k};x) f_{\mathsf{q}}^{(0)}(x)$$
$$= \alpha_{\mathsf{s}} \frac{C_F}{\pi}\left[-\frac{3}{4\varepsilon}\left(\frac{\Lambda^2}{\mu^2}\right)^\varepsilon + 2 + \mathcal{O}(\varepsilon)\right]\int_0^1 \mathrm{d}x$$
$$\times \int \mathrm{d}\boldsymbol{k} \, h_{\mathsf{b}}^{(0)}(\boldsymbol{k}) V_{\mathsf{q}}^{(0)}(\boldsymbol{k},x) f_{\mathsf{q}}^{(0)}(x) \,. \tag{78}$$

The remaining part is regular in the $\varepsilon \to 0$ limit and defines the finite term:

$$\frac{\mathrm{d}\sigma}{\mathrm{d}J}_{C_F}^{f,\text{finite}} := \alpha_{\mathsf{s}} \int_0^1 \frac{\mathrm{d}z}{z} \int \frac{\mathrm{d}\boldsymbol{l}}{\pi(\boldsymbol{l}-\boldsymbol{k})^2}\Big[I(z,\boldsymbol{l}) - I(0,\boldsymbol{l})$$
$$- \big(I(z,\boldsymbol{k}) - I(0,\boldsymbol{k})\big)\Theta(\Lambda^2 - (\boldsymbol{l}-\boldsymbol{k})^2)\Big] \tag{79}$$

This result (with explicit expressions for $I(z,\boldsymbol{k})$ etc.) will be used in our final formula.

Next we consider the term (i) with the **initial state** collinear singularity. We can write, in the same way as before,

$$\frac{\mathrm{d}\sigma}{\mathrm{d}J}_{C_F}^{i} := \alpha_{\mathsf{s}} \int_0^1 \frac{\mathrm{d}z}{z^{1-2\varepsilon}} \int \frac{\mathrm{d}\boldsymbol{l}}{\pi_\varepsilon \boldsymbol{l}^2} I(z,\boldsymbol{l})$$
$$= \frac{\mathrm{d}\sigma}{\mathrm{d}J}_{C_F}^{i,\text{soft}} + \frac{\mathrm{d}\sigma}{\mathrm{d}J}_{C_F}^{i,\text{coll}} + \frac{\mathrm{d}\sigma}{\mathrm{d}J}_{C_F}^{i,\text{finite}} \,, \tag{80}$$

where I is given by (76). One sees immediately that the soft contribution is exactly the same as for the (f) term:

$$\frac{\mathrm{d}\sigma}{\mathrm{d}J}_{C_F}^{i,\text{soft}} = \frac{\mathrm{d}\sigma}{\mathrm{d}J}_{C_F}^{f,\text{soft}} \,. \tag{81}$$

As to the collinear piece, we note that in the collinear limit $\boldsymbol{l} = 0$ the jet distribution reduces (by applying (49d)) to

$\mathcal{S}_J^{(2)}$, and one gets[4]

$$
\begin{aligned}
\frac{\mathrm{d}\sigma}{\mathrm{d}J}{}_{C_F}^{i,\mathrm{coll}} &:= \alpha_{\mathrm{s}} \int_0^1 \frac{\mathrm{d}z}{z^{1-2\varepsilon}} \int \frac{\mathrm{d}\boldsymbol{l}}{\pi_\varepsilon \boldsymbol{l}^2} \left[I(z,\boldsymbol{0}) - I(0,\boldsymbol{0}) \right] \\
&\quad \times \Theta(\Lambda^2 - \boldsymbol{l}^2) \\
&= \alpha_{\mathrm{s}} \frac{C_F}{2\pi} \int \mathrm{d}\boldsymbol{k}\, h_{\mathsf{b}}^{(0)}(\boldsymbol{k}) \frac{\mathcal{N} C_F}{\boldsymbol{k}^2} \int \frac{\mathrm{d}\boldsymbol{l}}{\pi_\varepsilon \boldsymbol{l}^2} \Theta(\Lambda^2 - \boldsymbol{l}^2) \\
&\quad \times \int_0^1 \mathrm{d}x\, f_{\mathsf{q}}^{(0)}(x) \int_0^1 \frac{\mathrm{d}z}{z^{1-2\varepsilon}} \\
&\quad \times \left[z \mathcal{P}_{\mathsf{gq}}(z,\varepsilon) \mathcal{S}_J^{(2)}(\boldsymbol{k};x(1-z)) - 2\mathcal{S}_J^{(2)}(\boldsymbol{k};x) \right] .
\end{aligned}
\tag{82}
$$

With the change of variable $z \to 1 - z$, and performing the $\boldsymbol{l}$ integration, we obtain

$$
\begin{aligned}
\frac{\mathrm{d}\sigma}{\mathrm{d}J}{}_{C_F}^{i,\mathrm{coll}} &= \alpha_{\mathrm{s}} \frac{C_F}{2\pi\varepsilon} \left(\frac{\Lambda^2}{\mu^2} \right)^\varepsilon \int \mathrm{d}\boldsymbol{k}\, h_{\mathsf{b}}^{(0)}(\boldsymbol{k}) h_{\mathsf{q}}^{(0)}(\boldsymbol{k}) \\
&\quad \times \int_0^1 \mathrm{d}x\, f_{\mathsf{q}}^{(0)}(x) \int_0^1 \mathrm{d}z\, \frac{1}{[(1-z)^{1-2\varepsilon}]_+} \\
&\quad \times \left[1 + z^2 + \varepsilon(1-z)^2 \right] \mathcal{S}_J^{(2)}(\boldsymbol{k};xz) ,
\end{aligned}
\tag{83}
$$

where the standard $()_+$ regularization has been used. To separate singular from finite pieces one has to perform an ε-expansion inside the z-integral. In order to cast the collinear singularity into the standard form, we introduce the full 4-dimensional Altarelli-Parisi $\mathsf{q} \to \mathsf{q}$ splitting function[5]

$$
\begin{aligned}
P_{\mathsf{qq}}(z) &= C_F \left(\frac{1+z^2}{1-z} \right)_+ \\
&= C_F \left[\frac{1+z^2}{(1-z)_+} + \frac{3}{2}\delta(1-z) \right].
\end{aligned}
\tag{84}
$$

We then can write

$$
\begin{aligned}
\frac{\mathrm{d}\sigma}{\mathrm{d}J}{}_{C_F}^{i,\mathrm{coll}} &= \alpha_{\mathrm{s}} \int \mathrm{d}\boldsymbol{k}\, h_{\mathsf{b}}^{(0)}(\boldsymbol{k}) \int_0^1 \mathrm{d}x\, f_{\mathsf{q}}^{(0)}(x) \\
&\quad \times \left\{ \frac{C_F}{\pi} \left(-\frac{3}{4\varepsilon} \right) \left(\frac{\Lambda^2}{\mu^2} \right)^\varepsilon V_{\mathsf{q}}^{(0)}(\boldsymbol{k},x) \right. \\
&\quad + \int_0^1 \mathrm{d}z\, V_{\mathsf{q}}^{(0)}(\boldsymbol{k},xz) \left[\frac{1}{\varepsilon} \left(\frac{\Lambda^2}{\mu^2} \right)^\varepsilon \frac{P_{\mathsf{qq}}(z)}{2\pi} \right. \\
&\quad \left. \left. + \frac{C_F}{\pi} \frac{1-z}{2} + \frac{C_F}{\pi} \left(\frac{\log(1-z)}{1-z} \right)_+ (1+z^2) \right] \right\} .
\end{aligned}
\tag{85}
$$

In the last expression the first term is again the LO jet cross section, multiplied by a singular factor; the second term contains the proper quark corrections to the quark

---

---

distribution function, while the remaining pieces are finite in the $\varepsilon \to 0$ limit.

The last contribution in the C_F part is regular in 4 dimensions and defines another finite term

$$
\begin{aligned}
\frac{\mathrm{d}\sigma}{\mathrm{d}J}{}_{C_F}^{i,\mathrm{finite}} &:= \alpha_{\mathrm{s}} \int_0^1 \frac{\mathrm{d}z}{z} \int \frac{\mathrm{d}\boldsymbol{l}}{\pi \boldsymbol{l}^2} \left[I(z,\boldsymbol{l}) - I(0,\boldsymbol{l}) \right. \\
&\quad \left. - \left(I(z,\boldsymbol{0}) - I(0,\boldsymbol{0}) \right) \Theta(\Lambda^2 - \boldsymbol{l}^2) \right]
\end{aligned}
\tag{86}
$$

and will be used in our final result.

4.4.2 C_A term

The term proportional to C_A in (72) reads

$$
\begin{aligned}
\frac{\mathrm{d}\sigma}{\mathrm{d}J}{}_{C_A} &= \alpha_{\mathrm{s}} \frac{C_A}{2\pi} \mathcal{N} C_F \int \mathrm{d}\boldsymbol{k}\, h_{\mathsf{b}}^{(0)}(\boldsymbol{k}) \int_0^1 \mathrm{d}x\, f_{\mathsf{q}}^{(0)}(x) \\
&\quad \times \int_{z_{\mathrm{cut}}}^1 \mathrm{d}z\, (1-z) \frac{\mathcal{P}_{\mathsf{gq}}(z,\varepsilon)}{\pi_\varepsilon} \\
&\quad \times \int \frac{\mathrm{d}\boldsymbol{k}'}{\boldsymbol{k}'^2} \frac{\boldsymbol{q} \cdot (\boldsymbol{q} - z\boldsymbol{k})}{\boldsymbol{q}^2 (\boldsymbol{q} - z\boldsymbol{k})^2} \mathcal{S}_J^{(3)}(\boldsymbol{k}',\boldsymbol{q},xz;x) \\
&= \frac{\mathrm{d}\sigma}{\mathrm{d}J}{}_{C_A}^{\mathrm{coll}} + \frac{\mathrm{d}\sigma}{\mathrm{d}J}{}_{C_A}^{\mathrm{LL}} + \frac{\mathrm{d}\sigma}{\mathrm{d}J}{}_{C_A}^{\mathrm{const}} .
\end{aligned}
\tag{87}
$$

It shows a $\mathsf{q} \parallel 1$ collinear singularity corresponding to the $\boldsymbol{k}' = 0$ pole. Because of the numerator, the $\boldsymbol{k}'$-integration is not really singular at $\boldsymbol{q} = 0$ nor at $\boldsymbol{q} - z\boldsymbol{k} = 0$, except for $z \to 0$. In fact, in the high energy limit (5), $\boldsymbol{q}$ fixed and $z \ll 1$ correspond to gluon 3 being in the central region, where we have

$$
\frac{C_A}{2\pi}(1-z) \frac{\mathcal{P}_{\mathsf{gq}}(z,\varepsilon)}{\pi_\varepsilon} \frac{\boldsymbol{q} \cdot (\boldsymbol{q} - z\boldsymbol{k})}{\boldsymbol{q}^2 (\boldsymbol{q} - z\boldsymbol{k})^2}
$$
$$
\xrightarrow{z \to 0} \frac{C_A}{\pi} \frac{1}{\pi_\varepsilon \boldsymbol{q}^2} \frac{1}{z} = K^{(0,\mathrm{real})}(\boldsymbol{k},\boldsymbol{k}') \frac{1}{z} .
\tag{88}
$$

This is exactly the expression entering the differential partonic cross section (22) in the central region that provides the LL contribution. In other words: (87) contains the $\mathsf{q} \parallel 1$ collinear singularity in the whole z-range; for finite values of z neither the $\mathsf{q} \parallel 3$ nor the $1 \parallel 3$ collinear singularities are really present. However, in the (gluon) central region $z \ll 1$ their "collinear denominators" degenerate, providing the soft singular real part of the leading kernel $\sim 1/\boldsymbol{q}^2$.

The jet distribution functions will become essential in disentangling the collinear singularities, the soft singularities, and the leading $\log s$ pieces. The basic mechanism can be understood as follows:

– When the outgoing quark 1 is in the collinear region of the incoming q, i.e., $y_1 \to \infty$, quark 1 cannot enter the jet; only gluon 3 can thus be the jet, y_3 is fixed and no logarithm of the energy can arise due to the lack of evolution in the gluon rapidity. No other singular configuration is found for the quark when $J = \{3\}$.

– In the composite jet configuration, i.e., $J = \{1, 3\}$, the gluon rapidity is bounded within a small range of values, and also in this case no $\log s$ can arise. There could be a singularity for vanishing gluon 3 momentum: even if the $1 \parallel 3$ collinear singularity is absent, we have seen that, at very low z, a soft singular integrand arises. However, the divergence is prevented by the jet cone boundary, which causes a shrinkage of the domain of integration $\sim z^2$ for $z \to 0$ and thus compensates the growth of the integrand.

– The one-quark jet configuration $J = \{1\}$ allows the gluon to span the whole phase space, apart, of course, from the jet region itself. The LL term arises from gluon configurations in the central region. But also here, like in the negative rapidity region discussed in Sect. 4.3, it is crucial to understand to what extent the differential cross section provides a leading contribution. It turns out that the coherence of QCD radiation suppresses the emission probability for gluon 3 rapidity y_3 being larger than the rapidity y_1 of the outgoing quark 1, and an angular ordering prescription similar to that of (65) holds. This will provide the final form of the leading term, i.e., the appropriate scale of the energy and, as a consequence, a finite and definite expression for the one-loop jet vertex correction.

As a first step we isolate, in (87), the initial state $\mathsf{q} \parallel 1$ collinear singular contribution and define, like in the C_F-term analysis, the collinear term by setting $\boldsymbol{k}' = 0$ (except in the $1/\boldsymbol{k}'^2$ pole), and by introducing an UV cutoff:

$$
\frac{\mathrm{d}\sigma}{\mathrm{d}J}{}^{\mathrm{coll}}_{C_A} := \alpha_{\mathrm{s}} \frac{C_A}{2\pi} \mathcal{N} C_F \int \mathrm{d}\boldsymbol{k}\, h_{\mathsf{b}}^{(0)}(\boldsymbol{k}) \int_0^1 \mathrm{d}x\, f_{\mathsf{q}}^{(0)}(x)
$$
$$
\times \int_{z_{\mathrm{cut}}}^1 \mathrm{d}z\, \mathcal{P}_{\mathsf{gq}}(z,\varepsilon) \int \frac{\mathrm{d}\boldsymbol{k}'}{\pi_\varepsilon \boldsymbol{k}'^2} \frac{\Theta(\Lambda^2 - \boldsymbol{k}'^2)}{\boldsymbol{k}^2}
$$
$$
\times \mathcal{S}_J^{(3)}(\boldsymbol{0}, \boldsymbol{k}, xz; x)\,. \tag{89}
$$

In this expression the jet distribution, because of (49c), reduces to $\mathcal{S}_J^{(2)}(\boldsymbol{k}; xz)$. By including the $\mathcal{N}C_A$ constant factors and the $1/\boldsymbol{k}^2$ pole, we reconstruct the *gluon-initiated* LO jet vertex (see (15) and (19)). Note also that

$$
C_F \mathcal{P}_{\mathsf{gq}}(z,\varepsilon) = C_F \frac{1 + (1-z)^2}{z} + C_F\, \varepsilon z
$$
$$
= P_{\mathsf{gq}}(z) + C_F\, \varepsilon z\,, \tag{90}
$$

where $P_{\mathsf{gq}}(z)$ is the 4-dimensional $\mathsf{q} \to \mathsf{g}$ splitting function. It will be used to define the quark correction to the *gluon* distribution function, and the lower bound z_{cut} can be set equal to zero (up to an error of the order t/s). The transverse integral is easily performed, and we obtain

$$
\frac{\mathrm{d}\sigma}{\mathrm{d}J}{}^{\mathrm{coll}}_{C_A} = \alpha_{\mathrm{s}} \int_0^1 \mathrm{d}x \int \mathrm{d}\boldsymbol{k}\, h_{\mathsf{b}}^{(0)}(\boldsymbol{k}) \int_0^1 \mathrm{d}z\, V_{\mathsf{g}}^{(0)}(\boldsymbol{k}, xz) f_{\mathsf{q}}^{(0)}(x)
$$
$$
\times \left[\frac{1}{\varepsilon} \left(\frac{\Lambda^2}{\mu^2} \right)^\varepsilon \frac{P_{\mathsf{gq}}(z)}{2\pi} + \frac{C_F}{\pi} \frac{z}{2} \right] + \mathcal{O}(\varepsilon)\,. \tag{91}
$$

By subtracting the collinear term (89) from the total C_A term (87), we obtain an expression, that is finite

in the $\varepsilon \to 0$ limit, and whose value increases logarithmically with s because of the $\mathrm{d}z/z$ integration with lower bound $z_{\mathrm{cut}} \sim s^{-1/2}$. As already mentioned, it is extremely important to understand the extension of the phase space contributing to the cross section at NLL accuracy, i.e., by including also the constant terms. That is actually crucial in the small-z region where the integrand develops a soft singularity which, if not properly absorbed in the real part of the kernel, could give rise to spurious divergencies spoiling the whole procedure.

It is instructive to review how the mechanism of suppression of the differential cross section sets in when the gluon is emitted at an angle smaller than that of the quark. At fixed quark momentum p_1, i.e., at fixed transverse momentum $\boldsymbol{k}' \neq 0$ and longitudinal momentum $p_1^3 \simeq (1-z)x\sqrt{s}/2$ – one can imagine $J = \{1\}$ fixed by the jet condition –, and at fixed gluon transverse energy $E_3 = |\boldsymbol{q}|$ and longitudinal momentum $p_3^3 \simeq xz\sqrt{s}/2$, we perform an azimuthal average of the subtracted C_A differential cross section with respect to the angle ϕ_3 of the gluon. The collinear subtraction actually does not contribute, because it refers to configuration with $\boldsymbol{k}' = 0$. If in this averaging procedure we neglect the variation of $h_{\mathsf{b}}^{(0)}(\boldsymbol{k})$, it is sufficient to calculate the azimuthal average of the factor

$$
\left\langle \frac{(1-z)\boldsymbol{q}\cdot(\boldsymbol{q} - z\boldsymbol{k})}{\boldsymbol{q}^2(\boldsymbol{q} - z\boldsymbol{k})^2} \right\rangle_{\phi_3} = \frac{1}{\boldsymbol{q}^2}\Theta(E_3 - z(E_1 + E_3))\,. \tag{92}
$$

This relation is exact and clearly shows that, outside the angular ordered region

$$
\frac{E_3}{z} > \frac{E_1}{1-z} \quad \Longleftrightarrow \quad \theta_3 > \theta_1 \quad \Longleftrightarrow \quad y_3 < y_1\,, \tag{93}
$$

there is no contribution to the cross section. In practice, by taking into account the variation of $h_{\mathsf{b}}^{(0)}(\boldsymbol{k})$ during the averaging procedure, we have to replace "no contribution" by "suppression". Note however that, in the limit $\boldsymbol{q} \to 0$ (which includes the soft region), the variation of $\boldsymbol{k}'$ goes to zero as well, so that (93) is really an accurate statement in the "dangerous" part of the phase space. Moreover, (92) shows that the $1/\boldsymbol{q}^2$ kinematic dependence of the LL kernel governs the differential cross section up to the very end of the angular boundary. Therefore, we define the LL contribution in the "lower half region" $y_3' > 0$ by

$$
\frac{\mathrm{d}\sigma}{\mathrm{d}J}{}^{\mathrm{LL}}_{C_A} := \alpha_{\mathrm{s}} \int \mathrm{d}\boldsymbol{k}\, h_{\mathsf{b}}^{(0)}(\boldsymbol{k}) \int \mathrm{d}\boldsymbol{k}'\, \frac{C_A}{\pi} \frac{1}{\pi_\varepsilon \boldsymbol{q}^2} h_{\mathsf{q}}^{(0)}(\boldsymbol{k}')
$$
$$
\times \int_{z_{\mathrm{cut}}}^1 \frac{\mathrm{d}z}{z}\, \Theta(E_3 - z(E_1 + E_3))
$$
$$
\times \int_0^1 \mathrm{d}x\, \mathcal{S}_J^{(2)}(\boldsymbol{k}', x) f_{\mathsf{q}}^{(0)}(x)
$$
$$
= \int_0^1 \mathrm{d}x \int \mathrm{d}\boldsymbol{k} \int \mathrm{d}\boldsymbol{k}'\, h_{\mathsf{b}}^{(0)}(\boldsymbol{k}) K^{(0,\mathrm{real})}(\boldsymbol{k}, \boldsymbol{k}')
$$
$$
\times \log\frac{\sqrt{xs}}{E_J + E_3} V_{\mathsf{q}}^{(0)}(\boldsymbol{k}', x) f_{\mathsf{q}}^{(0)}(x)\,, \tag{94}
$$

where we have imposed the $J = \{1\}$ jet condition.

Table 1. Schematics of the decomposition of real and virtual one-loop corrections to qb scattering and references of the corresponding equations

virtual				real								
$\omega^{(1)}$	$\widetilde{\Pi}_{\mathsf{q}}$	$\widetilde{\Pi}_{\mathsf{b}}$	$y_3' < 0$	$y_3' > 0$								
				C_F						C_A		
				f			i					
		$\underbrace{\qquad\qquad}$										
		$\swarrow \quad \searrow$										
LL	soft,coll	$h_{\mathsf{b}}^{(1)}$	LL	soft	coll	finite	soft	coll	finite	coll	LL	const
(96a)	(96b)	(68b)	(68a)	(77)	(78)	(79)	(81)	(85)	(86)	(91)	(94)	(95)

The remaining part of the C_A term is finite in 4 dimensions and constant in energy, so that we can set $\varepsilon = 0$ and $z_{\text{cut}} = 0$ to define the constant part

$$\frac{\mathrm{d}\sigma_{C_A}^{\text{const}}}{\mathrm{d}J} := \left[\frac{\mathrm{d}\sigma}{\mathrm{d}J}_{C_A} - \frac{\mathrm{d}\sigma_{C_A}^{\text{coll}}}{\mathrm{d}J} - \frac{\mathrm{d}\sigma_{C_A}^{\text{LL}}}{\mathrm{d}J} \right]_{\substack{z_{\text{cut}} = 0 \\ \varepsilon = 0}} . \quad (95)$$

5 The NLO jet vertex: Sum of real and virtual corrections

Having completed the calculation of both the virtual and real corrections in the whole phase space, we are going to collect all partial results and to show that the complete one-loop jet cross section can naturally be fitted to the form of (35). Table 1 summarizes the decomposition of the one-loop jet cross section and gives the references of the various contributions.

In Sect. 3 we have presented the virtual contributions to the jet cross section which, after renormalization of the coupling, assume the form of (44). We have already taken into account the contribution coming from the $\widetilde{\Pi}_{\mathsf{b}}$ impact factor correction in Sect. 4.3 by combining it with the "upper half region" real contribution in (68). The remaining virtual terms can be conveniently rewritten in the form

$$\left. \frac{\mathrm{d}\sigma^{(\text{virt})}}{\mathrm{d}J} \right|_{\omega^{(1)}} + \left. \frac{\mathrm{d}\sigma^{(\text{virt})}}{\mathrm{d}J} \right|_{\widetilde{\Pi}_{\mathsf{q}}}$$

$$= \alpha_s \int \mathrm{d}x \int \mathrm{d}\boldsymbol{k}\, \mathrm{d}\boldsymbol{k}'\, h_{\mathsf{b}}^{(0)}(\boldsymbol{k}) K^{(0,\text{virt})}(\boldsymbol{k}, \boldsymbol{k}')$$

$$\times \log \frac{xs}{s_0(\boldsymbol{k}, \boldsymbol{k}')} V_{\mathsf{q}}^{(0)}(\boldsymbol{k}', x) f_{\mathsf{q}}^{(0)}(x) \quad (96a)$$

$$+ \alpha_s \left[\left(\frac{E_J^2}{\mu^2} \right)^\varepsilon \left(-\frac{1}{\varepsilon^2} + \frac{3}{2\varepsilon} + \frac{\pi^2}{6} - 4 \right) \frac{C_F}{\pi} \right.$$

$$\left. + \left(\frac{85}{36} + \frac{\pi^2}{4} \right) \frac{C_A}{\pi} - \frac{5}{18} \frac{N_f}{\pi} - b_0 \log \frac{E_J^2}{\mu^2} \right]$$

$$\times \int \mathrm{d}x \int \mathrm{d}\boldsymbol{k}\, h_{\mathsf{b}}^{(0)}(\boldsymbol{k}) V_{\mathsf{q}}^{(0)}(\boldsymbol{k}, x) f_{\mathsf{q}}^{(0)}(x) , \quad (96b)$$

where the virtual kernel $K^{(0,\text{virt})}$ has been defined in (29) and the coefficient $\widetilde{\Pi}_{\mathsf{q}}$ is given in (45). The energy scale s_0 in (96a) is constrained to satisfy $s_0(\boldsymbol{k}, \boldsymbol{k}) = \boldsymbol{k}^2 = E_J^2$,

because the delta function inside the virtual kernel sets $\boldsymbol{k} = \boldsymbol{k}'$, and the delta function in the LO jet vertex sets $\boldsymbol{k}'^2 = E_J^2$. The general form of the energy scale for $\boldsymbol{k}' \neq \boldsymbol{k}$ will be fixed in a moment by the real LL contribution.

We first join the LL real contributions (68a) and (94): they show the same structure and differ only in the logarithmic term. The sum of the two logarithms yields

$$\log \frac{\sqrt{xs}}{\max(E_2, E_3)} + \log \frac{\sqrt{xs}}{E_J + E_3}$$

$$= \log \frac{xs}{(E_J + E_3)\max(E_2, E_3)} . \quad (97)$$

The denominator in the argument of the logarithm defines the energy scale s_0. However, as we have already pointed out, there is some freedom in choosing the LL subtraction and, correspondingly, the denominators in the $\log s$. We can obtain a more symmetric expression by defining the LL term in the "upper half region" as suggested at the end of Sect. 4.3: by replacing the scale $\max(E_2, E_3)$ by $E_2 + E_3$. This amounts to using the same prescription for defining the LL contribution in the "upper half region" $y_3' < 0$ and in the "lower half region" $y_3' < 0$. With this choice, the full LL contribution to the jet cross section, including the virtual correction (96a), is

$$\frac{\mathrm{d}\sigma^{\text{LL}}}{\mathrm{d}J} = \int \mathrm{d}x \int \mathrm{d}\boldsymbol{k}\, \mathrm{d}\boldsymbol{k}'\, h_{\mathsf{b}}^{(0)}(\boldsymbol{k}) K^{(0)}(\boldsymbol{k}, \boldsymbol{k}')$$

$$\times \log \frac{xs}{s_0(\boldsymbol{k}, \boldsymbol{k}')} V_{\mathsf{q}}^{(0)}(\boldsymbol{k}', x) f_{\mathsf{q}}^{(0)}(x) \quad (98)$$

$$s_0(\boldsymbol{k}, \boldsymbol{k}') := (|\boldsymbol{k}'| + |\boldsymbol{q}|)(|\boldsymbol{k}| + |\boldsymbol{q}|)$$

$$= (E_J + E_3)(E_2 + E_3) . \quad (99)$$

It is straightforward to check that

$$s_0(\boldsymbol{k}, \boldsymbol{k}') \to \boldsymbol{k}^2 = E_2^2 \qquad \text{for} \qquad \boldsymbol{k}^2 \gg \boldsymbol{k}'^2 , \quad (100\text{a})$$

$$s_0(\boldsymbol{k}, \boldsymbol{k}') \to \boldsymbol{k}'^2 = E_J^2 \qquad \text{for} \qquad \boldsymbol{k}^2 \ll \boldsymbol{k}'^2 , \quad (100\text{b})$$

$$s_0(\boldsymbol{k}, \boldsymbol{k}) = \boldsymbol{k}^2 = E_J^2 \qquad \text{for} \qquad \boldsymbol{k} = \boldsymbol{k}' . \quad (100\text{c})$$

These constraints are consequences of the QCD coherence effects [23]. We identify (98) with the first term of (35).

Let us stress that the energy scale in (99) – and in general all the scales satisfying (100) – arises naturally when one requires impact factors and PDFs to have standard collinear properties and the remaining non-leading-log term (95) to be finite in both the physical $\varepsilon \to 0$ and

high-energy $s \to \infty$ limits. Choosing a scale of the energy outside the class defined by (100) while preserving the above properties, requires the introduction of additional NLL operators (see (71)) which has to be added as multiplicative corrections to the Green's function. If, for instance, we adopt $s_0 = |\boldsymbol{k}||\boldsymbol{k}'|$, then the Green's function in (33b) has to be replaced by

$$
G(xs, \boldsymbol{k}, \boldsymbol{k}') = (\mathbf{1} + \alpha_{\mathrm{s}} H_L) \left[\mathbf{1} + \alpha_{\mathrm{s}} K^{(0)} \log \frac{xs}{|\boldsymbol{k}||\boldsymbol{k}'|} \right]
$$
$$
\times (\mathbf{1} + \alpha_{\mathrm{s}} H_R) \tag{101}
$$
$$
H_L(\boldsymbol{k}, \boldsymbol{k}') = -K^{(0)}(\boldsymbol{k}, \boldsymbol{k}') \log \frac{|\boldsymbol{k}| + |\boldsymbol{q}|}{|\boldsymbol{k}|} ,
$$
$$
H_R(\boldsymbol{k}, \boldsymbol{k}') = H_L(\boldsymbol{k}', \boldsymbol{k}) . \tag{102}
$$

The second term of (35) has already been obtained in (68b). We remark again that, with the choice of the energy scale (99), the one-loop impact factor correction $h_{\mathsf{b}}^{(1)}$ is no longer given by (69) but differs by a finite part. However, its actual expression is irrelevant for the jet vertex.

We now consider the sum of all ε-divergent contributions that have not been included in the $h_{\mathsf{b}}^{(1)}$ impact factor term (68b). They can be found in (96b,77,78,81,85,91) and add up to

$$
\frac{\mathrm{d}\sigma^{\mathrm{singular}}}{\mathrm{d}J} \tag{103}
$$
$$
= \frac{\alpha_{\mathrm{s}}}{2\pi} \frac{1}{\varepsilon} \left(\frac{\Lambda^2}{\mu^2} \right)^{\varepsilon} \int \mathrm{d}x \int \mathrm{d}\boldsymbol{k} \, h_{\mathsf{b}}^{(0)}(\boldsymbol{k}) V_{\mathsf{q}}^{(0)}(\boldsymbol{k}, x)
$$
$$
\times \left[P_{\mathsf{qq}} \otimes f_{\mathsf{q}}^{(0)} \right](x) + \frac{\alpha_{\mathrm{s}}}{2\pi} \frac{1}{\varepsilon} \left(\frac{\Lambda^2}{\mu^2} \right)^{\varepsilon}
$$
$$
\times \int \mathrm{d}x \int \mathrm{d}\boldsymbol{k} \, h_{\mathsf{b}}^{(0)}(\boldsymbol{k}) V_{\mathsf{g}}^{(0)}(\boldsymbol{k}, x) \left[P_{\mathsf{gq}} \otimes f_{\mathsf{q}}^{(0)} \right](x)
$$
$$
+ \alpha_{\mathrm{s}} \left[\left(\frac{3}{2} \log \frac{E_J^2}{\Lambda^2} - 2 \right) \frac{C_F}{\pi} + \left(\frac{85}{36} + \frac{\pi^2}{4} \right) \frac{C_A}{\pi} - \frac{5}{18} \frac{N_f}{\pi} \right.
$$
$$
\left. - b_0 \log \frac{E_J^2}{\mu^2} \right] \int \mathrm{d}x \int \mathrm{d}\boldsymbol{k} \, h_{\mathsf{b}}^{(0)}(\boldsymbol{k}) V_{\mathsf{q}}^{(0)}(\boldsymbol{k}, x) f_{\mathsf{q}}^{(0)}(x)
$$
$$
+ \alpha_{\mathrm{s}} \int \mathrm{d}x \int \mathrm{d}\boldsymbol{k} \, h_{\mathsf{b}}^{(0)}(\boldsymbol{k}) \int \mathrm{d}z \, V_{\mathsf{q}}^{(0)}(\boldsymbol{k}, xz) f_{\mathsf{q}}^{(0)}(x)
$$
$$
\times \left\{ \frac{C_F}{\pi} \left[\frac{1-z}{2} + \left(\frac{\log(1-z)}{1-z} \right)_+ (1+z^2) \right] + \frac{C_A}{\pi} \frac{z}{2} \right\} .
$$

All double poles have cancelled out. Single poles only appear in connection with the splitting functions: they are shown in the first three lines of (103), and they contribute to the third term of (35) which contains the PDF one-loop corrections. Note however that, since the present analysis has been restricted to the case of incoming quarks, we have obtained only the quark-initiated corrections to the quark and gluon PDF, i.e., only the term $\mathsf{c} = \mathsf{q}$ in the sum of (36). The gluon-initiated corrections require an incoming gluon out of hadron H and will be presented in a forthcoming paper [13]. It is also clear that the cutoff Λ can be identified with the factorization scale μ_F.

The last two terms of (103) are regular at $\varepsilon = 0$ and can be combined with the finite parts (79), (86) and (95).

The resulting expression can be cast into the form

$$
\frac{\mathrm{d}\sigma^{\mathrm{finite}}}{\mathrm{d}J} = \alpha_{\mathrm{s}} \int \mathrm{d}x \int \mathrm{d}\boldsymbol{k} \, h_{\mathsf{b}}^{(0)}(\boldsymbol{k}) V_{\mathsf{q}}^{(1)}(\boldsymbol{k}, x) f_{\mathsf{q}}^{(0)}(x) , \tag{104}
$$

which defines the NLO correction to the quark-initiated jet vertex

$$
V_{\mathsf{q}}^{(1)}(\boldsymbol{k}, x)
$$
$$
:= \left[\left(\frac{3}{2} \log \frac{\boldsymbol{k}^2}{\Lambda^2} - 2 \right) \frac{C_F}{\pi} + \left(\frac{85}{36} + \frac{\pi^2}{4} \right) \frac{C_A}{\pi} - \frac{5}{18} \frac{N_f}{\pi} \right.
$$
$$
\left. - b_0 \log \frac{\boldsymbol{k}^2}{\mu^2} \right] V_{\mathsf{q}}^{(0)}(\boldsymbol{k}, x) + \int \mathrm{d}z \, V_{\mathsf{q}}^{(0)}(\boldsymbol{k}, xz)
$$
$$
\times \left\{ \frac{C_F}{\pi} \left[\frac{1-z}{2} + \left(\frac{\log(1-z)}{1-z} \right)_+ (1+z^2) \right] + \frac{C_A}{\pi} \frac{z}{2} \right\}
$$
$$
+ \frac{C_A}{\pi} \int \frac{\mathrm{d}\boldsymbol{k}'}{\pi} \int \mathrm{d}z \left[\frac{1}{2} P_{\mathsf{qq}}(z) \left((1-z) \frac{\boldsymbol{q} \cdot (\boldsymbol{q} - \boldsymbol{k})}{\boldsymbol{q}^2 (\boldsymbol{q} - \boldsymbol{k})^2} h_{\mathsf{q}}^{(0)}(\boldsymbol{k}') \right. \right.
$$
$$
\times \mathcal{S}_J^{(3)}(\boldsymbol{k}', \boldsymbol{q}, xz; x) + - \frac{1}{\boldsymbol{k}'^2} \Theta(\Lambda^2 - \boldsymbol{k}'^2) V_{\mathsf{q}}^{(0)}(\boldsymbol{k}, xz)
$$
$$
\left. - \frac{1}{z\boldsymbol{q}^2} \Theta(|\boldsymbol{q}| - z(|\boldsymbol{q}| + |\boldsymbol{k}'|)) V_{\mathsf{q}}^{(0)}(\boldsymbol{k}', x) \right]
$$
$$
+ \frac{C_F}{2\pi} \int \mathrm{d}z \, \frac{1}{(1-z)_+} (1+z^2) \int \frac{\mathrm{d}\boldsymbol{l}}{\pi \boldsymbol{l}^2} \left[\frac{\mathcal{N} C_F}{\boldsymbol{l}^2 + (\boldsymbol{l} - \boldsymbol{k})^2} \right.
$$
$$
\times \left(\mathcal{S}_J^{(3)}(z\boldsymbol{k} + (1-z)\boldsymbol{l}, (1-z)(\boldsymbol{k} - \boldsymbol{l}), x(1-z); x) \right.
$$
$$
\left. + \mathcal{S}_J^{(3)}(\boldsymbol{k} - (1-z)\boldsymbol{l}, (1-z)\boldsymbol{l}, x(1-z); x) \right)
$$
$$
\left. - \Theta(\Lambda^2 - \boldsymbol{l}^2) \left(V_{\mathsf{q}}^{(0)}(\boldsymbol{k}, xz) + V_{\mathsf{q}}^{(0)}(\boldsymbol{k}, x) \right) \right] . \tag{105}
$$

It clearly depends on the jet definition and on three scales: the energy scale s_0 (via the subtraction of the LL term $\propto 1/z$), the factorization scale $\Lambda = \mu_F$ and the renormalization scale μ.

Equations (104) and (105) provide the fourth and last term of (35) and represent the main result of our study.

6 Conclusive remarks

In this paper we have investigated a particular class of jet final states in the high energy region. Both the theoretical and phenomenological motivation comes from the interest in the Regge limit of QCD: the jet production processes - forward jets in ep collisions and Mueller-Navelet jets in hadron-hadron collisions - have been designed to investigate BFKL dynamics at present and future colliders. Whereas the BFKL Pomeron is known at LO and NLO, a complete NLO analysis and comparison with data has not been possible, since neither the photon impact factor nor the jet vertex have been calculated in NLO. On the other hand, there is no doubt that at moderately large energies, NLO corrections to the asymptotic LO behaviour

are important for a reliable description of the processes under consideration. It is the purpose of this paper (and a forthcoming one) to calculate the jet vertex in NLO: in this first part we have studied the quark-initiated jet vertex, whereas the gluonic counterpart will be presented in a subsequent paper.

In order to extract the NLO jet vertex we have calculated the cross section of the process $quark\ \mathsf{b} + quark\ \mathsf{a} \rightarrow quark\ \mathsf{b} + X + jet$ at order α_s^3: apart from the NLO corrections to the impact factor of quark b and the contribution to gluon production in the central region, this process provides the NLO corrections to the quark-initiated vertex $quark\ \mathsf{a} \rightarrow jet$. As an important theoretical result we have verified that the factorization form (33a) holds: this proof follows from the fact that we have been able to separate, in the sum of virtual and real corrections, the collinear singularities which go into the renormalization of the parton density of the incoming quark a, and the gluon emission in the central region which is part of the LO calculation.

Another theoretical issue of interest is the dependence upon the scales. In leading order, results of the BFKL calculations and the jet vertex are insensitive to both the energy scale s_0 and to the renormalization scale μ. It is only at the NLO level that the dependence on these scales is being determined.

The central result of our calculation is the expression (105) for the NLO jet vertex. Using the factorization property (33a), we can use our result also for the upper incoming quark b, i.e., for the 'symmetric' Mueller-Navelet jet production process $\mathsf{q} + \mathsf{q} \rightarrow jet + X + jet$. As the final step, we will have to allow for the production of an arbitrary number of gluons between the jets which is described by the NLO BFKL Pomeron. This step will be presented in the companion paper containing the NLO gluon-initiated jet vertex.

With our expression for the jet vertex we have provided a finite integral that can be computed numerically, e.g. via Monte-Carlo integration. Such a numerical study requires to specify the jet algorithm described by the function $\mathcal{S}_J^{(3)}$: so far we have been rather general, but clearly the numerical results will depend on the choice of the jet algorithm.

References

1. L.N. Lipatov, Sov. J. Nucl. Phys. **23**, 338 (1976); E.A. Kuraev, L.N. Lipatov, V.S. Fadin, Sov. Phys. JETP **44**, 443 (1976); E.A. Kuraev, L.N. Lipatov, V.S. Fadin, Sov. Phys. JETP **45**, 199 (1977); Y. Balitskii, L.N. Lipatov, Sov. J. Nucl. Phys. **28**, 822 (1978)

2. J. Bartels, A. De Roeck, H. Lotter, Phys. Lett. B **389**, 742 (1996) [`hep-ph/9608401`]; S.J. Brodsky, F. Hautmann, D.E. Soper, Phys. Rev. D **56**, 6957 (1997) [`hep-ph/9706427`]

3. A.H. Mueller, H. Navelet, Nucl. Phys. B **282**, 727 (1987)

4. A.H. Mueller, Nucl. Phys. **B** (Proc. Suppl.) **18C**, 125 (1990); J. Phys. **G17**, 1443 (1991)

5. V. Del Duca, C.R. Schmidt, Phys. Rev. D **51**, 2150 (1995) [`hep-ph/9407359`]

6. J. Bartels, A. De Roeck, M. Loewe, Z. Physik C **54**, 635 (1992); J. Kwiecinski, A.D. Martin, P.J. Sutton, Phys. Rev. D **46**, 921 (1992); W.K. Tang, Phys. Lett. B **278**, 363 (1992)

7. V.S. Fadin, L.N. Lipatov, Phys. Lett. B **429**, 127 (1998) [`hep-ph/9802290`]

8. M. Ciafaloni, G. Camici, Phys. Lett. B **412**, 396 (1997) [`hep-ph/9707390`]; Phys. Lett. B **430**, 349 (1998) [`hep-ph/9803389`]

9. M. Ciafaloni, D. Colferai, G.P. Salam, Phys. Rev. D **60**, 114036 (1999) [`hep-ph/9905566`]

10. S.J. Brodsky, V.S. Fadin, V.T. Kim, L.N. Lipatov, G.B. Pivovarov, JETP Lett. **70**, 155 (1999) [`hep-ph/9901229`]

11. J. Bartels, S. Gieseke, C.-F. Qiao, Phys. Rev. D **63**, 056014 (2001) [`hep-ph/0009102`]; J. Bartels, S. Gieseke, A. Kyrieleis, Phys. Rev. D **65**, 014006 (2002) [`hep-ph/0107152`]

12. V.S. Fadin, A.D. Martin, Phys. Rev. D **60**, 114008 (1999) [`hep-ph/9904505`]; V.S. Fadin, D.Y. Ivanov, M.I. Kotsky, `hep-ph/0106099`

13. J. Bartels, D. Colferai, G.P. Vacca, in preparation

14. V.N. Gribov, L.N. Lipatov, Sov. J. Nucl. Phys. **15**, 438 (1972); G. Altarelli, G. Parisi, Nucl. Phys. B **126**, 298 (1977); Y.L. Dokshitzer, Sov. Phys. JETP **46**, 641 (1977)

15. See, e.g., J.R. Forshaw, D.A. Ross, Quantum Chromodynamics and the Pomeron, Cambridge University Press, 1997 and references therein

16. M. Ciafaloni, Phys. Lett. B **429**, 363 (1998) [`hep-ph/9801322`]

17. M. Ciafaloni, D. Colferai, Nucl. Phys. B **538**, 187 (1999) [`hep-ph/9806350`]

18. V.S. Fadin, R. Fiore, M.I. Kotsky, A. Papa, Phys. Rev. D **61**, 0 (2000)94005 and 094006 [`hep-ph/9908264` and `hep-ph/9908265`]

19. M. Ciafaloni, G. Rodrigo, JHEP **0005**, 042 (2000) [`hep-ph/0004033`]

20. See, e.g., J.C. Collins, D.E. Soper, G. Sterman in Perturbative QCD, World Scientific, Singapore, 1989 and references therein

21. V.S. Fadin, R. Fiore, A. Quartarolo, Phys. Rev. D **50**, 2265 (1994)

22. See, e.g., Z. Kunszt, D.E. Soper, Phys. Rev. D **46**, 192 (1992); S. Catani, M.H. Seymour, Nucl. Phys. B **485**, 291 (1997) [`hep-ph/9605323`]

23. M. Ciafaloni, Nucl. Phys. B **296**, 49 (1988)

24. S. Catani, M. Ciafaloni, F. Hautman, Nucl. Phys. B **366**, 135 (1991)